

University of Windsor

## Scholarship at UWindor

---

Electronic Theses and Dissertations

Theses, Dissertations, and Major Papers

---

1-1-1970

### Charge transfer spectra of square planar d(8) transition metal complexes.

John L. H. Batiste  
*University of Windsor*

Follow this and additional works at: <https://scholar.uwindsor.ca/etd>

---

#### Recommended Citation

Batiste, John L. H., "Charge transfer spectra of square planar d(8) transition metal complexes." (1970). *Electronic Theses and Dissertations*. 6078.  
<https://scholar.uwindsor.ca/etd/6078>

This online database contains the full-text of PhD dissertations and Masters' theses of University of Windsor students from 1954 forward. These documents are made available for personal study and research purposes only, in accordance with the Canadian Copyright Act and the Creative Commons license—CC BY-NC-ND (Attribution, Non-Commercial, No Derivative Works). Under this license, works must always be attributed to the copyright holder (original author), cannot be used for any commercial purposes, and may not be altered. Any other use would require the permission of the copyright holder. Students may inquire about withdrawing their dissertation and/or thesis from this database. For additional inquiries, please contact the repository administrator via email ([scholarship@uwindsor.ca](mailto:scholarship@uwindsor.ca)) or by telephone at 519-253-3000ext. 3208.

CHARGE TRANSFER SPECTRA OF SQUARE PLANAR  
 $d^8$  TRANSITION METAL COMPLEXES

BY

JOHN L. H. BATISTE

A DISSERTATION

Submitted to the Faculty of Graduate Studies through the  
Department of Chemistry in Partial Fulfillment  
of the Requirements for the Degree of  
Doctor of Philosophy at the  
University of Windsor

Windsor, Ontario

1970

UMI Number: DC52645

### INFORMATION TO USERS

The quality of this reproduction is dependent upon the quality of the copy submitted. Broken or indistinct print, colored or poor quality illustrations and photographs, print bleed-through, substandard margins, and improper alignment can adversely affect reproduction.

In the unlikely event that the author did not send a complete manuscript and there are missing pages, these will be noted. Also, if unauthorized copyright material had to be removed, a note will indicate the deletion.

**UMI**<sup>®</sup>

---

UMI Microform DC52645

Copyright 2008 by ProQuest LLC.

All rights reserved. This microform edition is protected against unauthorized copying under Title 17, United States Code.

ProQuest LLC  
789 E. Eisenhower Parkway  
PO Box 1346  
Ann Arbor, MI 48106-1346

ADX 5265

THIS DISSERTATION HAS BEEN EXAMINED AND APPROVED BY:

Don A. Martin

Edwin J. Bunnell  
Chairman

C. E. Linn

W. J. Schaefer

Robert C. Penfold

321912

## ABSTRACT

Electronic spectra of some anions ( $\text{Cl}^-$ ,  $\text{Br}^-$ ,  $\text{I}^-$ ,  $\text{SCN}^-$ , and  $\text{CN}^-$ ) and of several complexes of the type  $[\text{MX}_4]^{2-}$  ( $\text{M} = \text{Pd(II)}$ ,  $\text{Pt(II)}$ ;  $\text{X} = \text{Cl}^-$ ,  $\text{CN}^-$ ) were recorded in water and deuterium oxide to a lower wavelength limit of 170  $\text{m}\mu$ . Improved resolution was obtained via the use of short pathlength cells. Complexes of the type  $[\text{MX}_4]^{n-}$  ( $\text{M} = \text{Pd(II)}$ ,  $\text{Pt(II)}$ ,  $\text{Au(III)}$ ;  $\text{X} = \text{Cl}^-$ ,  $\text{Br}^-$ ,  $\text{CN}^-$ ) were also examined to the 170  $\text{m}\mu$  limit in acetonitrile. A trial and error Gaussian analysis of the spectra was aided by a low temperature ( $168^\circ\text{K}$ ) thin film technique. Trends in the high frequency bands are discussed. The halide complexes show ligand  $\rightarrow$  metal charge transfer bands and metal  $\rightarrow$  ligand charge transfer bands at even higher energy. The cyanide complexes exhibit both d-d and metal  $\rightarrow$  ligand charge transfer bands.

The electronic spectrum of  $\text{Pt(en)Cl}_2$  was examined in water and deuterium oxide.

## ACKNOWLEDGEMENTS

It is a pleasure to acknowledge the aid, guidance, and encouragement of Dr. R. C. Rumfeldt without whose talent and insight this work would not have been possible.

Gratitude is expressed to the National Research Council of Canada for the studentship awarded to me during the course of this work.

A special vote of thanks goes to Mary, my thoughtful and very patient wife.

## TABLE OF CONTENTS

	Page
Abstract	ii
Acknowledgements	iii
List of Tables	v
List of Figures	vi
Introduction	1
Experimental	17
Preparation of Compounds	20
Spectral Measurements	23
Results	28
Discussion	59
Appendix <b>I, II</b>	74, <b>81</b>
Bibliography	<b>83</b>
Vita Auctoris	<b>85</b>

LIST OF TABLES

Table	Title	Page
I	Transition Intensities for Various Types of Complexes	2
II	Electronic Transitions in Square Planar Halide Complexes	11
III	Electronic Transitions in Square Planar Cyanide Complexes	13
IV A&B	Chemical Suppliers	18-19
V	Solution Spectra of $\text{Cl}^-$ , $\text{Br}^-$ , $\text{I}^-$	32
VI	Spectra Subjected to Gaussian Analysis	37
VII	Electronic Spectra of Square Planar Chloride Complexes	45
VIII	Electronic Spectra of Square Planar Bromide Complexes	49
IX	Electronic Spectra of Square Planar Cyanide Complexes	53
X	Electronic Spectrum of $\text{Pt(en)Cl}_2$	58
XI	Ligand Field Parameters for Square Planar Complexes	65
XII	Electronic Spectrum of $\text{Pt}(\text{NH}_3)_4^{2+}$	71
XIII	Electronic Spectra of $\text{PtCl}_4^{2-}$ and $\text{PdCl}_4^{2-}$	75
XIV	Electronic Spectra of Square Planar Halide Complexes	76
XV	Electronic Spectra of Square Planar Cyanide Complexes	79
XVI	Comparison of Computed and Observed Spectral Band Frequencies	80



LIST OF FIGURES

Figure	Title	Page
1	Molecular Orbital Diagram for Square Planar Halide Complexes	10
2	Molecular Orbital Diagram for Square Planar Cyanide Complexes	12
3	Construction of Thin Cells	24
4	Dependence of Slit Width on Frequency; Electronic Spectrum of H <sub>2</sub> O	26
5	Electronic Spectrum of KCl	29
6	Electronic Spectrum of KBr	30
7	Electronic Spectrum of KI	31
8	Electronic Spectrum of KSCN	34
9	Electronic Spectrum of KCN	35
10	Solvent Dependence of the High Frequency Electronic Spectrum of Pt Cl <sub>4</sub> <sup>2-</sup>	39
11	Electronic Spectrum of PtCl <sub>4</sub> <sup>2-</sup> in H <sub>2</sub> O	40
12	Electronic Spectrum of PtCl <sub>4</sub> <sup>2-</sup> in CH <sub>3</sub> CN	41
13	Electronic Spectrum of Pd(CN) <sub>4</sub> <sup>2-</sup> Thin Film Sample on Quartz Plate	42
14	Electronic Spectrum of Pd <sub>2</sub> Cl <sub>6</sub> <sup>2-</sup> in CH <sub>3</sub> CN	43
15	Electronic Spectrum of AuCl <sub>4</sub> <sup>1-</sup> in CH <sub>3</sub> CN	44
16	Electronic Spectrum of PtBr <sub>4</sub> <sup>2-</sup> in CH <sub>3</sub> CN	46
17	Electronic Spectrum of Pd <sub>2</sub> Br <sub>6</sub> <sup>2-</sup> in CH <sub>3</sub> CN	47
18	Electronic Spectrum of AuBr <sub>4</sub> <sup>1-</sup> in CH <sub>3</sub> CN	48
19	Electronic Spectrum of Pt(CN) <sub>4</sub> <sup>2-</sup> in CH <sub>3</sub> CN	50
20	Electronic Spectrum of Pd(CN) <sub>4</sub> <sup>2-</sup> in CH <sub>3</sub> CN	51
21	Electronic Spectrum of Au(CN) <sub>4</sub> <sup>1-</sup> in CH <sub>3</sub> CN	52

Figure	Title	Page
22	Molecular Orbital Diagram for Dichloroethylenediamine-platinum (II)	56
23	Electronic Spectrum of Pt (en) Cl <sub>2</sub>	57

## INTRODUCTION

This laboratory's interest in coordination complexes with  $d^8$  electronic configuration and belonging to the  $D_{4h}$  symmetry group stemmed from the observation that hydrated electrons were produced in the low wavelength (1849 Å) photolysis of aqueous  $PtCl_4^{2-}$ .

Photochemistry is the study of the chemical actions initiated by excited states formed by the absorption of light. Any discussion of the extremely complex events which can occur after the primary excitation requires the existence of a reasonable assignment of the electronic transitions, especially in the spectral region of the photolysis.

To a first approximation the electronic transitions in coordination compounds may be classified in the following way: 1) ligand field transitions, 2) charge transfer transitions, and 3) intra-ligand transitions. The last type is not likely to be observed except for those cases in which the ligands have their own  $\pi$  systems. As can be seen in Table I, the intensities of the various transitions are dependent upon the type of electronic transition, the electronic configuration, the coordination symmetry, and the type of ligand.

Ligand field excited states originate from electronic transitions between orbitals mainly localized on the central metal. From an electrostatic viewpoint these transitions amount to an angular redistribution of the electronic charge at the central metal, yielding an increase in electronic density along the coordination directions with a corresponding decrease in some directions between the ligands. The results are increased repulsion between the central metal and ligands and improved ease of

TABLE I

Transition Intensities for Various Types of Complexes<sup>1</sup>

Extinction Coefficient ( $M^{-1} \text{ cm}^{-1}$ )	Type of Transition <sup>a</sup>	Type of Complex
$10^{-2} - 1$	Spin forbidden Laporte forbidden	Many octahedral and tetrahedral complexes of $d^5$ ions - e.g. $\text{Mn}(\text{H}_2\text{O})_6^{2+}$
$1 - 10$	Spin forbidden Laporte forbidden	Tetrahedral complexes of $d^5$ ions with intensity stealing - e.g. $\text{MnBr}_4^{2-}$
		Spin forbidden bands of transition metal ions in general
	Spin allowed Laporte forbidden	Ionic six coordinate molecules - e.g. $\text{Ni}(\text{H}_2\text{O})_6^{2+}$
$10 - 10^2$	Spin forbidden Laporte forbidden	Certain of the more covalent tetrahedral complexes of $d^5$ ions - e.g. $\text{FeBr}_4^{1-}$
	Spin allowed Laporte forbidden	Six coordinate molecules with intensity stealing; complexes with organic ligands.
		Some square planar complexes - e.g. $\text{PdCl}_4^{2-}$
$10^2 - 10^3$	Spin allowed Laporte forbidden	Many tetrahedral complexes - e.g. $\text{NiCl}_4^{2-}$ Certain six coordinate molecules of very low symmetry - e.g. $(2\text{-picoline})_2\text{Co}(\text{NO}_3)_2$ Many square planar complexes, particularly with organic ligands
	Spin allowed Laporte allowed	Some charge transfer bands (M-L) in molecules with unsaturated ligands
$10^2 - 10^4$	Spin allowed Laporte forbidden	Certain six coordinate complexes with ligands such as acetylacetonate

Table I (contd.)

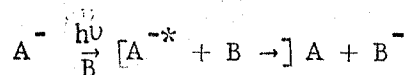
Extinction Coefficient ( $M^{-1} \text{ cm}^{-1}$ )	Type of Transition <sup>a</sup>	Type of Complex
$10^3 - 10^6$	Spin allowed Laporte allowed	Many charge transfer absorptions. Electronically allowed transitions in aromatic molecules.

<sup>a</sup> The absorption bands concerned are assumed to be essentially d - d, crystal field, unless otherwise stated.

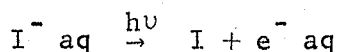
nucleophilic attack at the central metal by solvent molecules or other ligands present in solution. Therefore ligand field excited states would be expected to favour substitution reactions (e.g. hydrolysis).

Charge transfer excited states originate from electronic transitions between molecular orbitals mainly localized on the central metal and molecular orbitals mainly localized on the ligands. One type of charge transfer excitation is charge transfer from the ligand to the metal (CTLM). A subdivision into two classes can be made: a) charge transfer from  $\pi$  nonbonding to metal anti-bonding d orbitals, and b) charge transfer from  $\sigma$  bonding to metal anti-bonding d orbitals. The nominal reduction in bond order in case (a) is 0.5. Most probably this class of transition will have the same chemical consequence as the ligand field transition (i.e. heterolytic fission --hydrolysis). However there is no basis to expect that the quantum efficiency of hydrolysis initiated by the  $\pi^n \rightarrow \sigma^*$  excitation will be the same as that resulting from ligand field excitation. In fact the quantum efficiency in the charge transfer case may possibly be greater than that in the ligand field case due to the reduction in bond order. Removing an electron from  $\sigma^b$  and placing it in a  $d^*$  orbital in case (b) nominally reduces the bond order by 1.0. The chemical effect which may be reasonably anticipated is a homolytic bond fission (i.e. a free radical or redox reaction). A second type of charge transfer excitation is charge transfer from metal to ligand (CTML). Both of these types of transitions give rise to a radial redistribution of the electronic charge between the central metal and the ligands. Consequently the charge transfer excited states in these cases would be expected to lead to intramolecular oxidation - reduction reactions. Charge transfer transitions between the complex and other species

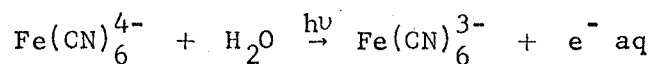
may also occur. This group would of course include charge transfer to solvent (CTTS).



The excited state of  $A^-$  would have an electron in an orbital of relatively low effective nuclear charge, and the binding energy of the electron would be reduced. Thus if the electron affinity of solvent B was greater than that of  $A^*$ , electron transfer could occur. These excited states would be anticipated to yield intermolecular oxidation - reduction reactions. An example is the CTTS transition for iodide ion in water<sup>2</sup>.



It is interesting that CTTL transitions may correlate strongly with CTTS transitions; the excitation via CTTL would approximate the process  $L^z \rightarrow L^{z-1}$  where  $L^{z-1}$  should have a low effective ionization potential. An example is the production of a photoelectron and an oxidized complex consequent upon the flash photolysis<sup>3</sup> of the CTTL band of  $\text{Fe}(\text{CN})_6^{4-}$ :



It is tempting to explain the photochemistry of transition metal complexes on the basis of the following double correlation: irradiation of charge transfer bands  $\rightarrow$  oxidation reduction reactions, irradiation of ligand field bands  $\rightarrow$  substitution reactions. On the other hand,

Balzani et al<sup>4</sup> feel that there is no experimental justification to draw a correlation between the type of irradiation and the type of photo-reaction observed, "This (i.e. the experimental data) indicates that in most cases the excited state directly reached with the irradiation may undergo a radiationless deactivation before having the chance to react. In this way an excited state having a different chemical reactivity may be obtained." This conclusion was drawn with respect to  $\text{PtCl}_4^{2-}$  where photoaquation was found to be the only result regardless of whether the ligand field bands or the charge transfer bands were irradiated.<sup>5</sup> The photolysis of  $\text{PtCl}_4^{2-}$  was carried out at 254, 313, 404 and 472 m $\mu$  to yield  $\text{PtCl}_3(\text{H}_2\text{O})^{1-}$  with quantum efficiencies of 0.65, 0.13, and 0.14 and 0.14 respectively.

However when the most recent interpretations<sup>6,7,8</sup> of the aqueous spectrum of  $\text{PtCl}_4^{2-}$  were compared with a Gaussian analysis performed in this laboratory, the results indicated doubt as to whether the absorption frequency at  $39,370 \text{ cm}^{-1}$  (254 m $\mu$ ) was ligand field or charge transfer in character. The lack of bond order change and the likelihood of inter-system crossing in ligand field excited states make it possible for the quantum efficiency to be the same for different d-d excitation wavelengths. On the other hand, for  $\pi^n \rightarrow d^*$  excitation, the quantum efficiency may be different even though the product is the same.

It is this author's opinion that it is too early to compare ligand field and charge transfer band photolyses, especially in square planar complexes where so little has been done with regard to spectral interpretation of charge transfer bands.<sup>9</sup>

As Basch points out,<sup>10</sup> molecular orbital theory is the most realistic method of treatment of transition metal complexes where there



exists the possibility of overlap, covalency, and electron exchange between metal and ligand. The use of Group Theory facilitates the construction of a qualitative picture of the molecular orbitals which describe the bonding in a complex. The key connection between Group Theory and chemical bonding lies in the following statement<sup>11</sup>, "If a molecule belongs to a certain symmetry Group, then the wave functions which describe the molecule must possess the same transformation properties under the symmetry operations of the Group as do the irreducible representations of the Group." In short, the molecule or complex is assigned to a point Group and using vectors to represent the  $\sigma$  bonds and possible  $\pi$  bonds as the basis, the irreducible representations to which the  $\sigma$  and  $\pi$  molecular orbitals belong are derived. From the transformation properties of the molecular orbitals the proper linear combination of ligand and metal atomic orbitals to construct these molecular orbitals can be determined. It is customary to label such orbitals and wave functions by the symbols associated with the irreducible representations according to which they transform. Convention requires that small letters be employed for orbitals and that capital letters be used for term wave functions. The term wave function for any particular state, be it the ground state or an excited state, is derived by taking the direct product of the irreducible representations of the partially filled orbitals. The intensity of an absorption band resulting from an electric dipole transition between a pair of states a and b depends on the magnitude of the integral<sup>12</sup>:

$$\int \psi_b^* m \psi_a d\tau = m_{ba}$$

where  $\psi_b^*$  and  $\psi_a$  are the total wave functions of states b and a respectively,

$m$  is the electric dipole moment operator,

$m_{ba}$  is the transition moment, and for which

$|m_{ba}|^2$  is the dipole strength of the transition.

The conditions under which the integral fails to vanish for the various possible pairs of states of a given system are known as selection rules.

A transition between a pair is said to be forbidden if  $m_{ba}$  vanishes.

At times a first approximation to the correct wave functions a and b

will show  $m_{ba} = 0$ , whereas a higher approximation will lead to a non-

vanishing value of the transition moment. These transitions are said

to be approximately forbidden. If the precise wave functions show  $m_{ba}$

to be zero, then the transition is labelled strictly forbidden. In

terms of Group Theory, for the transition moment to be non-zero, the

direct product of the representations of the initial and final wave

functions with the particular dipole moment operator component must

contain the totally symmetric representation. Since each dipole moment

operator component transforms as a translation, it has odd (u) parity.

In order to obtain a symmetric (g) representation in the total direct

product, it is necessary that the direct product of the representations of the initial and final state wave functions should be odd ( $u \times u = g$ ).

Thus the selection rule called Laporte's Rule is derived. Transitions

between states of the same parity are forbidden ( $\Delta l = \pm 1$ ; e.g. d $\rightarrow$ d).

For negligible spin-orbit interaction, the electronic wave function can

be approximately factorized into orbital  $\psi_e^o$  and spin  $\psi_e^s$  components:

$$\psi_e = \psi_e^o \cdot \psi_e^s$$

Since the electric dipole moment operator does not involve spin, we can re-write the expression for the transition moment as:

$$\int \psi_a^O m \psi_b^O d v \int \psi_a^S \psi_b^S d s$$

If the ground and excited state wave functions do not have the same spin, the second integral vanishes due to spin orthogonality. Hence transitions between wave functions of different spin are forbidden ( $\Delta S = 0$ )<sup>1</sup>

Figures 1 and 2 are molecular orbital diagrams for square planar halide and cyanide complexes respectively. Tables II and III summarize the various orbital and term transitions. It must be borne in mind that the molecular orbital diagrams are qualitative in nature. They indicate which atomic orbitals can be taken in linear combinations to form the requisite molecular orbitals, but not the relative contributions of each atomic orbital. The ordering, which has been chosen so as to conform with the latest published views<sup>6,7,8,13,14</sup> is again qualitative.

The most recent summary<sup>8</sup> of the interpretations of the electronic spectra of  $\text{Pt Cl}_4^{2-}$  and  $\text{Pd Cl}_4^{2-}$  in aqueous solution is given in Table XIII in the Appendix I. The majority of the effort has been directed towards sorting out the ligand field transitions. The case of  $\text{Pt Cl}_4^{2-}$  serves as an example to illustrate the techniques employed to give support to the assignments. The single crystal absorption at  $26,300 \text{ cm}^{-1}$  was assigned to the  ${}^1A_{2g}$  excited state because of its xy polarization.<sup>6,7,15</sup> From the results of magnetic circular dichroism studies<sup>16,17</sup>, the  $30,300 \text{ cm}^{-1}$  absorption of  $\text{PtCl}_4^{2-}$  was assigned as the transition to the  ${}^1E_g$  state. The transition seen at  $36,500 \text{ cm}^{-1}$  in the diffuse reflectance spectrum<sup>18</sup> was assigned to the  ${}^1B_{1g}$  excited state. The first high intensity band

Figure 1

Figure 1

Molecular Orbital Diagram for Square  
Planar Halide Complexes

Molecular Orbital Diagram  
 $D_{4h}$  halide  
 ligands

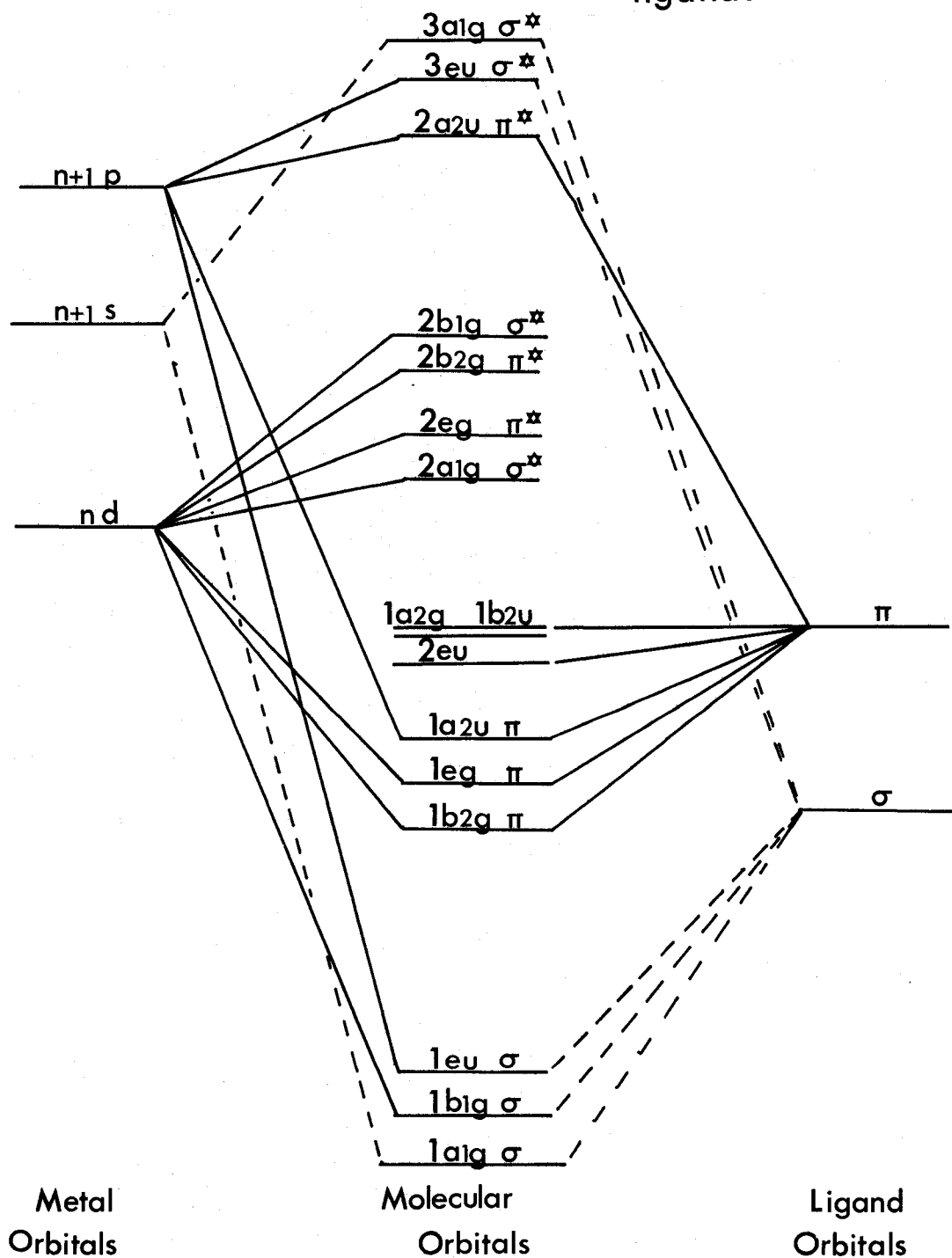


TABLE II

Electronic Transitions in Square Planar  
Halide Complexes

Orbital Transition	Term Transition
$2b_{2g}^* \uparrow 2b_{1g}^*$	${}^1A_{1g} \uparrow {}^1A_{2g}$
$2e_g^* \uparrow 2b_{1g}^*$	$\uparrow {}^1E_g$
$2a_{1g}^* \uparrow 2b_{1g}^*$	$\uparrow {}^1B_{1g}$
$1b_{2u}(\pi^n) \rightarrow 2b_{1g}^*$	$\rightarrow {}^1A_{2u}$
$2e_u(\pi^n) \rightarrow 2b_{1g}^*$	$\rightarrow {}^1E_u(1)$
$1a_{2u}(\pi^b) \uparrow 2b_{1g}^*$	$\uparrow {}^1B_{2u}$
$1e_u(\sigma^b) \rightarrow 2b_{1g}^*$	$\rightarrow {}^1E_u(2)$
$2b_{2g}^* \uparrow 2a_{2u}^*$	$\uparrow {}^1B_{1u}$
$2e_g^* \rightarrow 2a_{2u}^*$	$\rightarrow {}^1E_u(3)$
$2a_{1g}^* \rightarrow 2a_{2u}^*$	$\rightarrow {}^1A_{2u}$
$2b_{2g}^* \rightarrow 3e_u^*$	$\rightarrow {}^1E_u(4)$
$2e_g^* \rightarrow 3e_u^*$	$\rightarrow \cancel{{}^1A_{1u}}, \cancel{{}^1A_{2u}}, \cancel{{}^1B_{1u}}, \cancel{{}^1B_{2u}}$
$2a_{1g}^* \rightarrow 3e_u^*$	$\rightarrow {}^1E_u(5)$

Figure 2



Figure 2

Molecular Orbital Diagram for Square  
Planar Cyanide Complexes

Molecular Orbital Diagram  
 $D_{4h}$   $CN^-$  Ligands

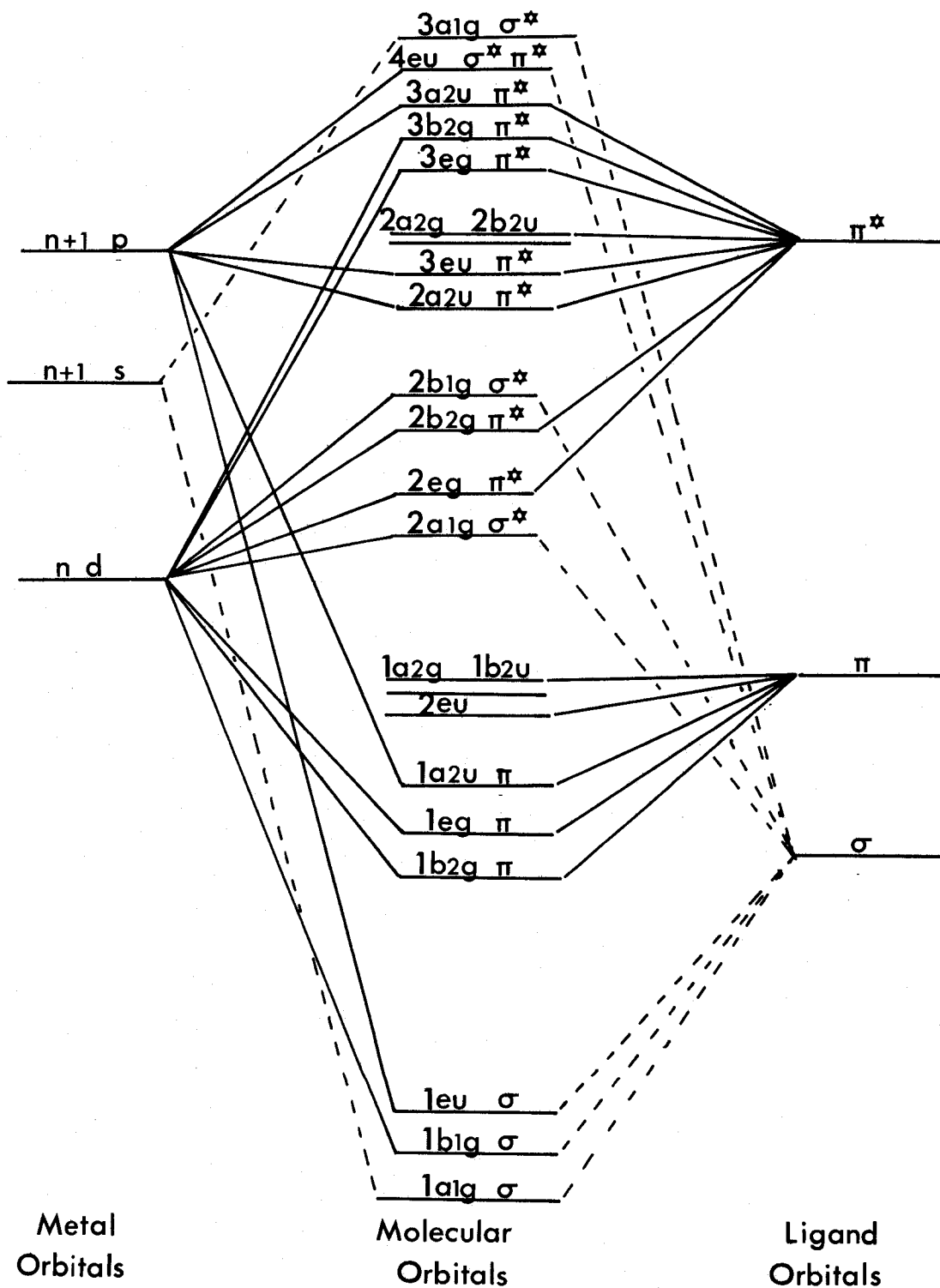


TABLE III

Electronic Transitions in Square  
Planar Cyanide Complexes

Orbital Transition	Term Transition
$2b_{2g}^* \uparrow 2b_{1g}^*$	${}^1A_{1g} \uparrow {}^1A_{2g}$
$2e_g^* \uparrow 2b_{1g}^*$	$\uparrow {}^1E_g$
$2a_{1g}^* \uparrow 2b_{1g}^*$	$\uparrow {}^1B_{1g}$
$2b_{2g}^* \uparrow 2a_{2u}^*$	$\uparrow {}^1B_{1u}$
$2e_g^* \rightarrow 2a_{2u}^*$	$\rightarrow {}^1E_u(3)$
$2a_{1g}^* \rightarrow 2a_{2u}^*$	$\rightarrow {}^1A_{2u}$
$2b_{2g} \rightarrow 3e_u^*$	$\rightarrow {}^1E_u(4)$
$2e_g^* \rightarrow 3e_u^*$	$\rightarrow \cancel{A_{1u}}, \cancel{A_{2u}}, \cancel{B_{1u}}, \cancel{B_{2u}}$
$2a_{1g}^* \rightarrow 3e_u^*$	$\rightarrow {}^1E_u(5)$
$2b_{2g}^* \uparrow 2b_{2u}^*$	$\uparrow {}^1A_{1u}$
$2e_g^* \rightarrow 2b_{2u}^*$	$\rightarrow {}^1E_u(6)$
$2a_{1g}^* \uparrow 2b_{2u}^*$	$\uparrow {}^1B_{2u}$

in  $\text{PtCl}_4^{2-}$  and  $\text{PdCl}_4^{2-}$  has been assumed to be due to the charge transfer transition  $\pi^n \rightarrow b_{1g}^*$ . The intense transition in  $\text{PdCl}_4^{2-}$  at still higher frequency ( $44,900 \text{ cm}^{-1}$ ) has been assigned to the  $\sigma^b \rightarrow b_{1g}^*$  process; however, the analogous transition in  $\text{PtCl}_4^{2-}$  had not been reported.

In order to extend the comparison, Mason and Gray<sup>19,14</sup> also looked at the chloride complex of gold (III), and both the bromide and cyanide complexes of platinum (II), palladium (II), and gold (III). Non-aqueous solvents were utilized to avoid the hydrolysis problems which plague these complexes. The results and assignments are summarized in Tables XIV and XV in the Appendix I. Much of this work centred on the ligand field transitions and sought to correlate frequency trends with changes in the central metal ion and the ligand. Increased attention was focussed on the charge transfer bands with attempts to draw correlations similar to those in the ligand field spectra. Unfortunately the spectral studies were restricted to wavelengths greater than 200 - 210 m $\mu$ .

Of late, several semiempirical molecular orbital calculations of electronic structure<sup>7,8,13,20</sup> have been carried out for square planar complexes with special emphasis on  $\text{PtCl}_4^{2-}$ . Some of Basch's results<sup>10</sup> are summarized in Table XVI in the Appendix I. He used a cyclic self-consistent charge and configuration approach. The parameters involved in the calculation were evaluated by fitting the frequency of the first observed charge transfer band to the computed value. Generally there is good agreement between the calculated ligand field transition frequencies and the observed values. However the agreement falls off in the second charge transfer transitions. It is the actual choice of valence orbital ionization potentials, wave functions, and Wolfsberg-Helmholz K factors

which determines the calculated properties of the complexes. Even though one set of parameters may be superior, there is no unambiguous method to establish this set by the simple molecular orbital treatment. Also 'since the numbers of interest to us here (electronic spectra) are of the same order of magnitude as the inherent error in the theory upon which the computations are based, significance can be attached only to consistent behaviour within a group of molecules'<sup>10</sup>.

It is not the intention here to detract from the usefulness of the theoretical approach and to promote the value of the experimental. Suffice it to say that the limitations in the theoretical approach combined with experimental data which is not absolutely complete allow adequate room for co-existence.

In spite of the valuable contributions made by these recent efforts, the band structure of  $\text{PtCl}_4^{2-}$  in the  $1849 \text{ \AA}$  region remains unexplained. The use of 1.00 cm path cells precluded spectra of aqueous solutions of much detail below  $200 \text{ m}\mu$ . The addition of chloride ion to inhibit the hydrolysis of  $\text{Pd Cl}_4^{2-}$  only intensified the problem by raising the ultra-violet cutoff point. Non-aqueous solvents in 1.00 cm path cells likewise possessed unfavourable cutoffs: acetonitrile,  $190 \text{ m}\mu$ ; ether-isopentane - ethanol (EPA),  $212 \text{ m}\mu$ ; 2-methyltetrahydrofuran - methanol,  $244 \text{ m}\mu$ ; 2 - methyltetrahydrofuran - propionitrile,  $238 \text{ m}\mu$ .

The objective of the present research was to examine and interpret the band structure of  $\text{PtCl}_4^{2-}$  in the spectral region of  $1849 \text{ \AA}$ . The use of short pathlength cells promised to be a means of exploring the region of interest. Comparison of spectra run in water, deuterium oxide, and acetonitrile served to point out which transitions were more strongly solvent - dependent. Since the interpretation of the electronic

spectrum of one complex is but an isolated statement, the study was extended to examine the chloride, bromide, and cyanide complexes of platinum (II), palladium (II), and gold (III) so that spectral frequency trends could substantiate the assignments. It was felt that the replacement of the potassium counter-ion in the various complexes with the tetra-n-butylammonium ion would reduce the crystallinity of some salts to the extent where a thin film deposited on a quartz plate would be suitable for spectral purposes. It was found that if sufficient care was exercised the stability of the thin film allowed its reduction in temperature with the consequence of further improvement in resolution.

Another reason for inquiry into higher frequency spectral regions lay in the anomalous appearance of a split  $E_u$  state in the cyanide complexes of platinum (II) and palladium (II). One author<sup>14</sup> has explained this as 'ion pairing in the solvent'.

Another author<sup>21</sup> has attributed the splitting to second order spin-orbit effects.

Using calculations based on magnetic circular dichroism (MCD) studies Piepho, Schatz, and McCaffery<sup>30</sup> have derived assignments for the electronic absorption spectrum of  $\text{Pt}(\text{CN})_4^{2-}$  which differ significantly from either that presented by Mason and Gray<sup>14</sup> or that to be presented here. A brief discussion of their conclusions appears in Appendix II.

It was felt that a more complete spectral picture of these complexes might allow the assignment of all the observed bands without resorting to these rather unique explanations.

## EXPERIMENTAL

The materials in Tables **IV** were purchased and used without additional purification.

TABLE IV<sub>A</sub>  
Chemical Suppliers

Chemical	Source of Supply	Comment
Potassium Chloride, KCl	J.T. Baker Chemicals	A.C.S. Grade
Potassium Bromide, KBr	B.D.H. Laboratory Chemicals	A.C.S. Grade Analytical Reagent
Potassium Iodide, KI	Fisher Scientific Company	A.C.S. Grade
Potassium Thiocyanate, KSCN	Mallinckrodt Chemicals	Analytical Reagent
Potassium Cyanide, KCN	Fisher Scientific Company	A.C.S. Grade
Deuterium Oxide, D <sub>2</sub> O	Merck, Sharp, and Dohme	Isotopic Purity 99.7 Atom % D
Acetonitrile, CH <sub>3</sub> CN	Fisher Scientific Company	Boiling Range 81.4 <sup>o</sup> - 82.8 <sup>o</sup> C H <sub>2</sub> O = 0.2 %



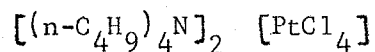
TABLE IV  
B

## Chemical Suppliers

Chemical	Source of Supply
Tetra-butylammonium Chloride, $(n-C_4H_9)_4 NCl$	Eastman Organic Chemicals
Tetra-n-butylammonium Bromide, $(n-C_4H_9)_4 N Br$	Eastman Organic Chemicals
Potassium Tetrachloroplatinate (II), $K_2PtCl_4$	Fisher Scientific Company
Potassium Hexachloroplatinate (IV), $K_2PtCl_6$	Fisher Scientific Company
Potassium Tetracyanoplatinate (II), $K_2Pt(CN)_4$	Research Inorganic Chemicals
Potassium Tetrachloropalladate (II), $K_2PdCl_4$	Alfa Inorganics
Potassium Tetracyanopalladate (II), $K_2Pd(CN)_4$	K & K Laboratories Rare and Fine Chemicals
Dichloroethylenediamineplatinum (II) $Pt(en)Cl_2$	D.F. Goldsmith Chemicals
Hydrogen Tetrachloroaurate (III), (Chloroauric Acid), $HAuCl_4 \cdot 3H_2O$	Fisher Scientific Company
Potassium Dicyanoaurate (I), $KAu(CN)_2$	K & K Laboratories Rare and Fine Chemicals

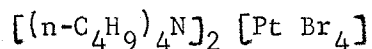
PREPARATION OF COMPOUNDS

Tetra-n-butylammonium Tetrachloroplatinate (II).



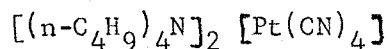
A saturated aqueous solution containing 0.2 g of  $K_2PtCl_4$  was treated with a saturated aqueous solution containing a 10% less than stoichiometric amount of tetra-n-butylammonium chloride. The resulting solution was extracted with 30 ml of chloroform. Evaporation of the chloroform yielded a thick oil which was dissolved in dichloromethane. The dichloromethane was removed by rotary evaporation to leave a red solid which was vacuum dried in a desiccator.

Tetra-n-butylammonium Tetrabromoplatinate (II),



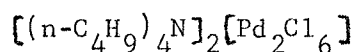
A saturated aqueous solution containing 0.2 g  $K_2PtCl_4$  was treated with 2.0 ml concentrated HBr (48.2%) and was evaporated to a volume of not less than 1 ml. This process was repeated twice more to expel most of the remaining HCl. A saturated aqueous solution containing a stoichiometric amount of tetra-n-butylammonium bromide was added dropwise at ice-bath temperature. A greenish-grey precipitate formed slowly. This precipitate was collected, washed with cold water, washed with ether, and then dried under vacuum.

Tetra-n-butylammonium Tetracyanoplatinate (II),



This compound was prepared according to the method of W.R. Mason and H.B. Gray<sup>14</sup>.

Tetra-n-butylammonium Tetrachloro- $\mu, \mu'$ -dichloro-dipalladate (II),

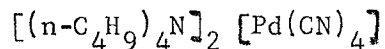


A saturated aqueous solution containing 0.2 g of  $K_2PdCl_4$  was treated with a saturated aqueous solution containing a stoichiometric amount of tetra-n-butylammonium chloride. A reddish precipitate formed immediately. This precipitate was collected, washed with cold water, washed with ether, and finally dried under vacuum.

Tetra-n-butylammonium Tetrabromo- $\mu, \mu'$ -dibromo-dipalladate (II),  $[(n-C_4H_9)_4N]_2$   
 $[Pd_2Br_6]$

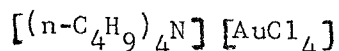
A saturated aqueous solution containing 0.2 g of  $K_2PdCl_4$  was treated with 2.5 ml. concentrated HBr (48.2%) and was evaporated to a small volume (1 ml). This process was repeated twice more to expel most of the remaining HCl. The resulting solution was extracted with 25 ml of methylene chloride containing a 10% less than stoichiometric amount of tetra-n-butylammonium bromide. The organic phase was evaporated to a volume of not less than 1 ml and was cooled to produce a crystalline precipitate. This product was collected, washed with ether, and dried under vacuum.

Tetra-n-butylammonium Tetracyanopalladate (II),



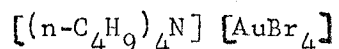
This compound was prepared according to the procedure of W.R. Mason and H.B. Gray<sup>14</sup>.

Tetra-n-butylammonium Tetrachloroaurate (III),



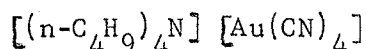
This compound was prepared according to the method of W.R. Mason and H.B. Gray<sup>19</sup>.

Tetra-n-butylammonium Tetrabromoaurate (III),



This compound was prepared according to the procedure of W.R. Mason and H.B. Gray<sup>19</sup>.

Tetra-n-butylammonium Tetracyanoaurate (III),



The method of J.M. Smith and co-workers<sup>22</sup> was employed to prepare  $KAu(CN)_2Br_2 \cdot 2H_2O$  from 0.5 g of the starting material  $KAu(CN)_2$ .

To prepare  $Au(CN)_4^{1-}$ , a stoichiometric amount of KCN was dissolved in the minimum amount of methanol. The solid yellow needles of  $KAu(CN)_2Br_2 \cdot 2H_2O$  were added slowly at ice-bath temperature. The colour gradually faded away and a fine white precipitate appeared. The methanolic solution was carefully evaporated to dryness. The white solid so obtained [a mixture of  $KAu(CN)_4$  and KBr] was dissolved in several ml of water. To this solution was added slowly dropwise a saturated aqueous solution containing a stoichiometric amount of tetra-n-butylammonium bromide. The fine white precipitate which was formed immediately was washed with cold water, washed with ether, and finally dried under vacuum.

## SPECTRAL MEASUREMENTS

A Beckman Model DK-1A prism-type instrument equipped with  $\text{MgF}_2$ -coated mirrors was employed to obtain electronic spectra in deuterium oxide, acetonitrile, and quadruply-distilled water<sup>\*</sup> to the low wavelength limit of 170  $\mu$ .

As the spectral wavelength was decreased, the detector was changed at 400  $\mu$  from a lead sulfide unit to a photomultiplier; at 350  $\mu$  the lamp source was switched from tungsten to deuterium. At wavelengths below 200  $\mu$  the photomultiplier was operated at a twenty-fold increase in sensitivity, and the cell compartment was vigorously purged with high purity nitrogen to minimize light absorption by atmospheric gases. Purging also served to limit the heating of the sample compartment.

Quartz cells with pathlength of 1.00 cm were obtained from Beckman and from Hellma. The 0.4375 cm path cells were purchased from Hellma.

Cell paths of 0.010 cm and 0.0074 cm  $\pm$  3 % were achieved through a Beckman Variable Path U.V. Cell (Research and Industrial Instrument Company) equipped with Suprasil quartz windows. Calibration was effected via a solution of  $\text{K}_2\text{PtCl}_6$  of known concentration ( $\epsilon_{262} = 24,500^{23}$ )

A cell with path of 0.028 cm  $\pm$  3 % was prepared by the University of Windsor glassblower, W. Eberhart ( See Figure 3). A pathlength of 0.028 cm was achieved by hand-grinding the RZ 11 glass spacer to a point where further grinding appeared to effect no further decrease in slit width. The surface tension operating principle restricted its use to aqueous solutions.

Spectral measurements in solution were carried out at room temperature

\* Doubly-distilled water served equally as well.

FIGURE 3

FIGURE 3

Construction of Thin Cells

Path = 0.028 cm.

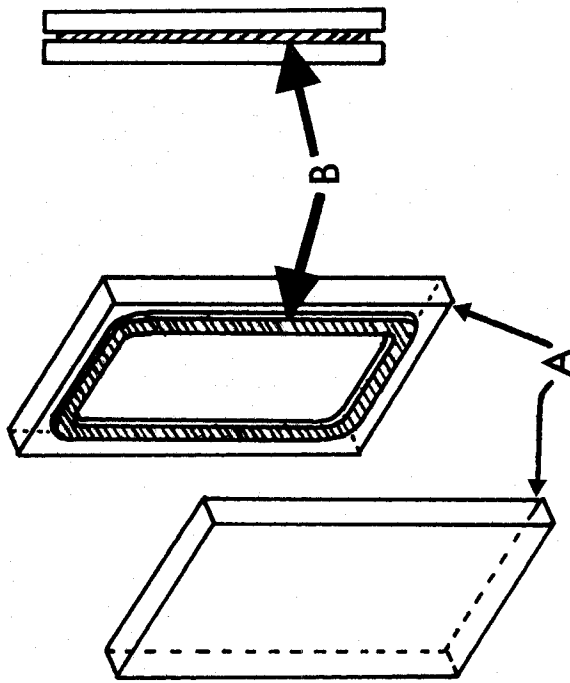
A = Suprasil Quartz Plates

Height = 45 mm

Width = 14 mm

Thickness = 1.5 mm

B = RZ II Glass





(22° - 24°C). Based on an average of seven determinations, the precision in the calculation of the extinction coefficient ( $M^{-1} \text{ cm}^{-1}$ ) at high frequencies was found to be  $\pm 5\%$ .

It is recognized that stray light is a potential problem, increasing in importance as source lamp intensity decreases. The appearance of spurious bands at high frequency can be a consequence of stray light, thus the  $55,400 \text{ cm}^{-1}$  band in the spectrum of  $\text{PtCl}_4^{2-}$  in  $\text{H}_2\text{O}$  may be suspect. The dependence of slit width on frequency for water, deuterium oxide, acetonitrile, and thin film samples is illustrated in Figure 4. It is possible to interpret the plateau in slit width for solution samples above  $57,500 \text{ cm}^{-1}$  as a result of decreasing source lamp intensity combined with a fairly constant intensity of stray light. However there is an alternate explanation for the slit width plateau which allows the  $55,400 \text{ cm}^{-1}$  band of aqueous  $\text{PtCl}_4^{2-}$  to be genuine. Instrument specifications claim less than 1% stray light at  $175 \text{ m}\mu$  ( $57,471 \text{ cm}^{-1}$ ). Slit width behaviour for solution samples is explainable in terms of a falloff in source lamp intensity combined with decreasing solvent absorption; the spectrum of water (pathlength = 0.028 cm) is plotted in Figure 4 for comparison. The lack of a plateau in slit width for thin film samples supports this explanation. It is also important that the  $55,400 \text{ cm}^{-1}$  band in  $\text{H}_2\text{O}$  shifts to  $56,200 \text{ cm}^{-1}$  in  $\text{D}_2\text{O}$  and disappears in  $\text{CH}_3\text{CN}$ . If the  $55,400 \text{ cm}^{-1}$  band were due to stray light, a more consistent pattern would be expected throughout the spectra of the complexes examined. Stray light effects can be important; however, there is no conclusive evidence that it is, or is not, making an important contribution here.

FIGURE 4

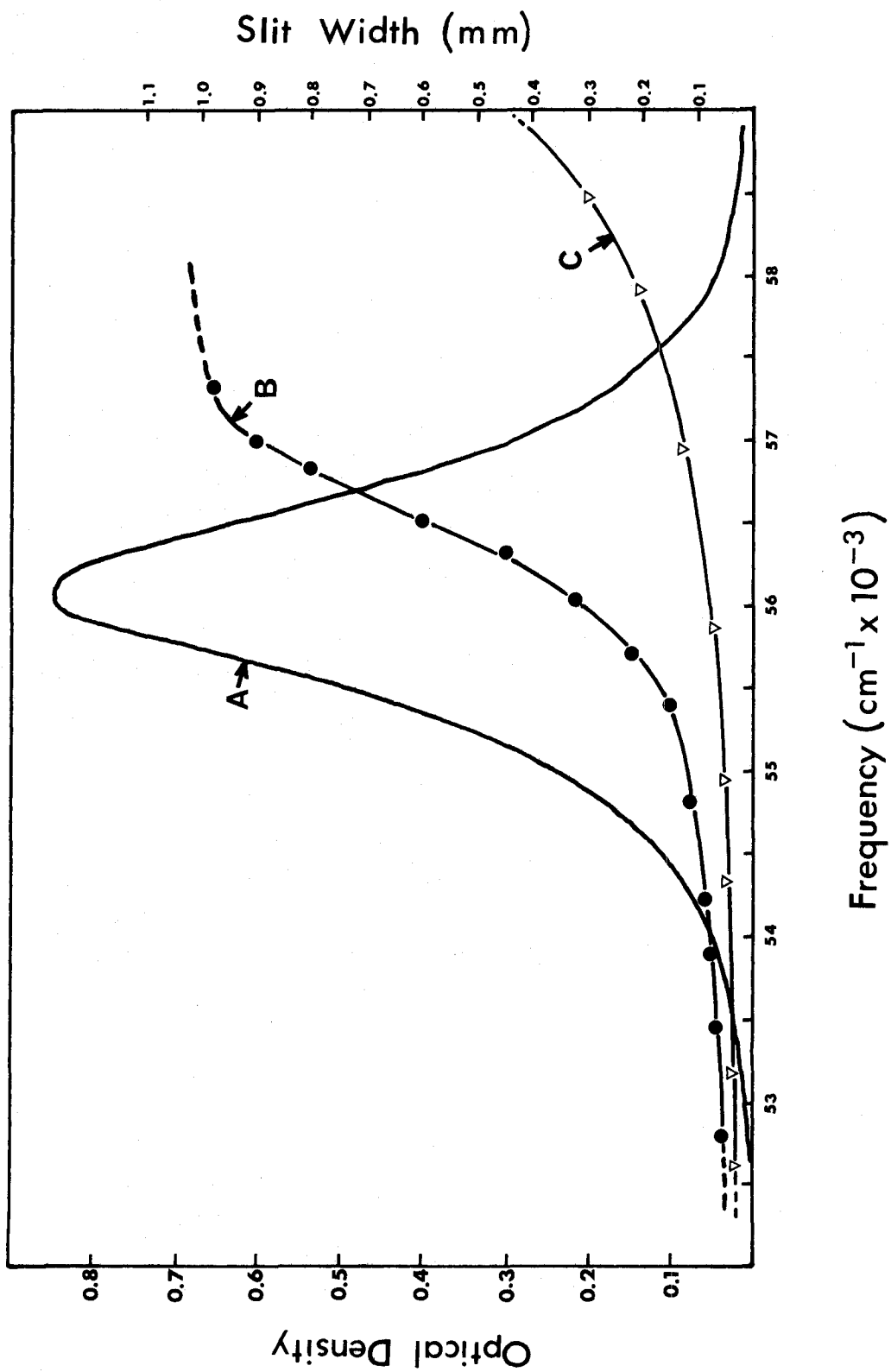
FIGURE 4

Dependence of Slit Width on Frequency

A Electronic spectrum of  $\text{H}_2\text{O}$  for path length ( $b$ ) = 0.028 cm

B Slit width vs frequency for  $\text{H}_2\text{O}$  and  $\text{D}_2\text{O}$  ( $b = 0.028$  cm) and  $\text{CH}_3\text{CN}^2$  ( $b = 0.010, 0.0074$  cm)

C Slit width vs frequency for quartz plate



Thin film samples were prepared by allowing a dichloromethane solution of the compound to evaporate on a quartz plate. Electronic spectra of the thin film samples were recorded at room temperature and also at reduced temperature with the aid of an Air Products Cryo-Tip Model AC-1-110 equipped with a vacuum shroud Model WMX-17. Temperatures were determined by a copper-constantan thermocouple. The usual tip temperature was  $86^{\circ} - 87^{\circ}\text{K}$ , whereas the plate temperature was approximately  $168^{\circ}\text{K}$ .

Gaussian analyses of the spectra were effected by a trial and error technique based on the criterion of the smallest possible number of smooth symmetrical peaks. The smallest possible number was sought since it is always possible to decompose any Gaussian curve into a larger number of smaller Gaussian curves. The expectation of smooth, symmetrical components was based on the appearance of the  $^2\text{P}_{3/2}$  transition of KI in  $\text{H}_2\text{O}$ . Adherence to the Gaussian equation  $\epsilon = \epsilon_{\text{MAX}} \exp \left[ -\left(\frac{w}{\theta}\right)^2 \right]$  was checked by testing the relationship  $h = 1.6651 \theta$ . Generally speaking, the value of  $h$  for the resolved peaks was equal to  $1.6651 \theta$  to within 5 - 6%. Positions of maxima of the resolved components are dependable to 200 - 300  $\text{cm}^{-1}$ .

## RESULTS

The electronic spectra of KCl, KBr, and KI are depicted in Figures 5, 6, and 7 respectively. The separations between the resolved components are compared in Table V with the published figures for the doublet splitting between the ground states of the respective halogen atoms in gas phase. The trend in spectral frequencies of the CTTS bands,  $\text{Cl}^- > \text{Br}^- > \text{I}^-$ , is in agreement with the ionization potentials.

FIGURE 5

Figure 5

Electronic Spectrum of KCl.

— Spectrum in  $H_2O$

Concentration (c) =  $4.29 \times 10^{-3} M$

Pathlength (b) = 0.028 cm

.. Resolved components of spectrum in  $H_2O$

-- Spectrum in  $D_2O$

c =  $4.40 \times 10^{-3} M$

b = 0.028 cm



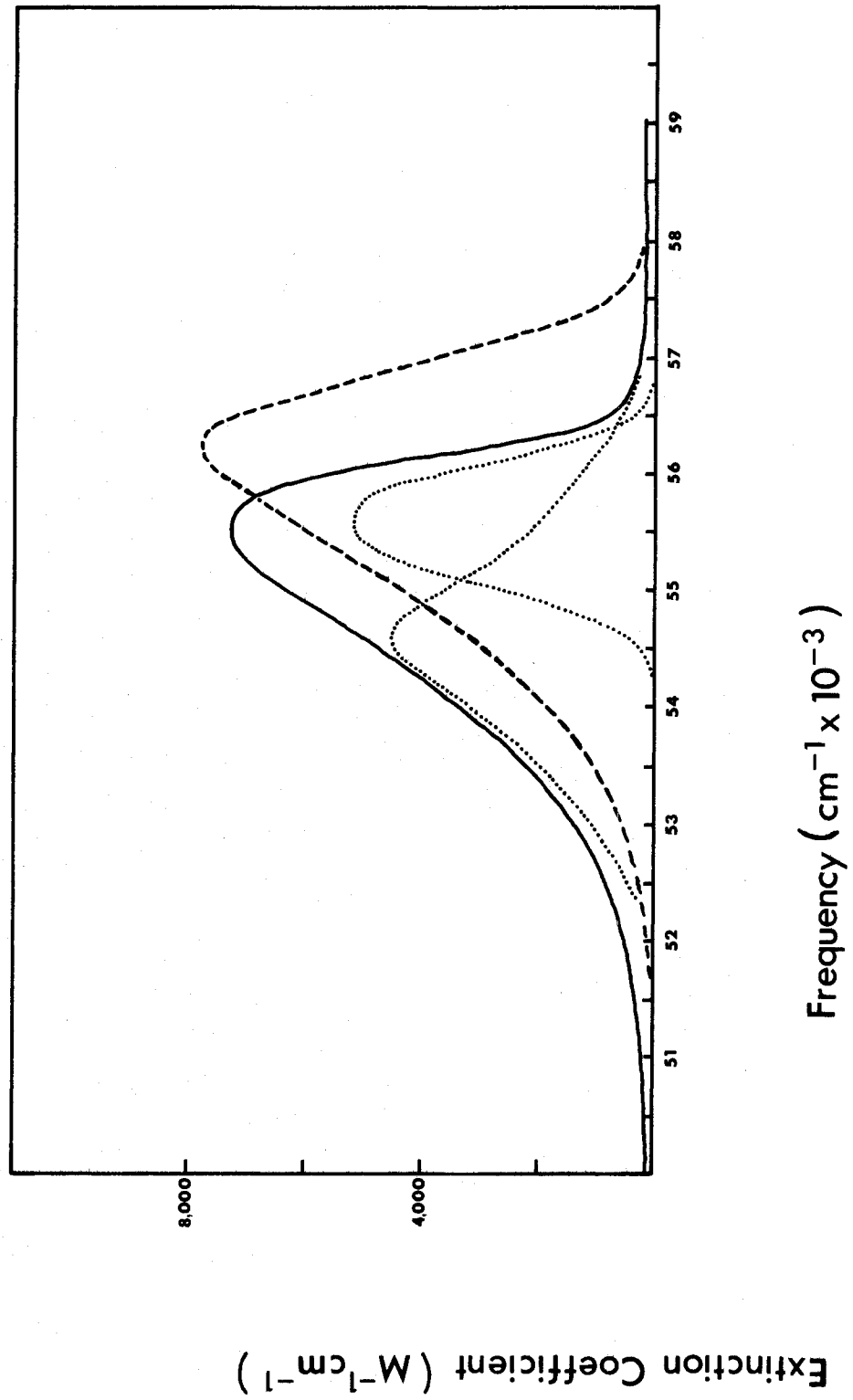


FIGURE 6

Figure 6

Electronic Spectrum of KBr

— Spectrum in  $\text{H}_2\text{O}$

$$c = 2.1 \times 10^{-3} \text{M}$$

$$b = 0.028 \text{ cm}$$

.. Resolved components of spectrum in  $\text{H}_2\text{O}$

-- Spectrum in  $\text{D}_2\text{O}$

$$c = 2.29 \times 10^{-3} \text{M}$$

$$b = 0.028 \text{ cm}$$

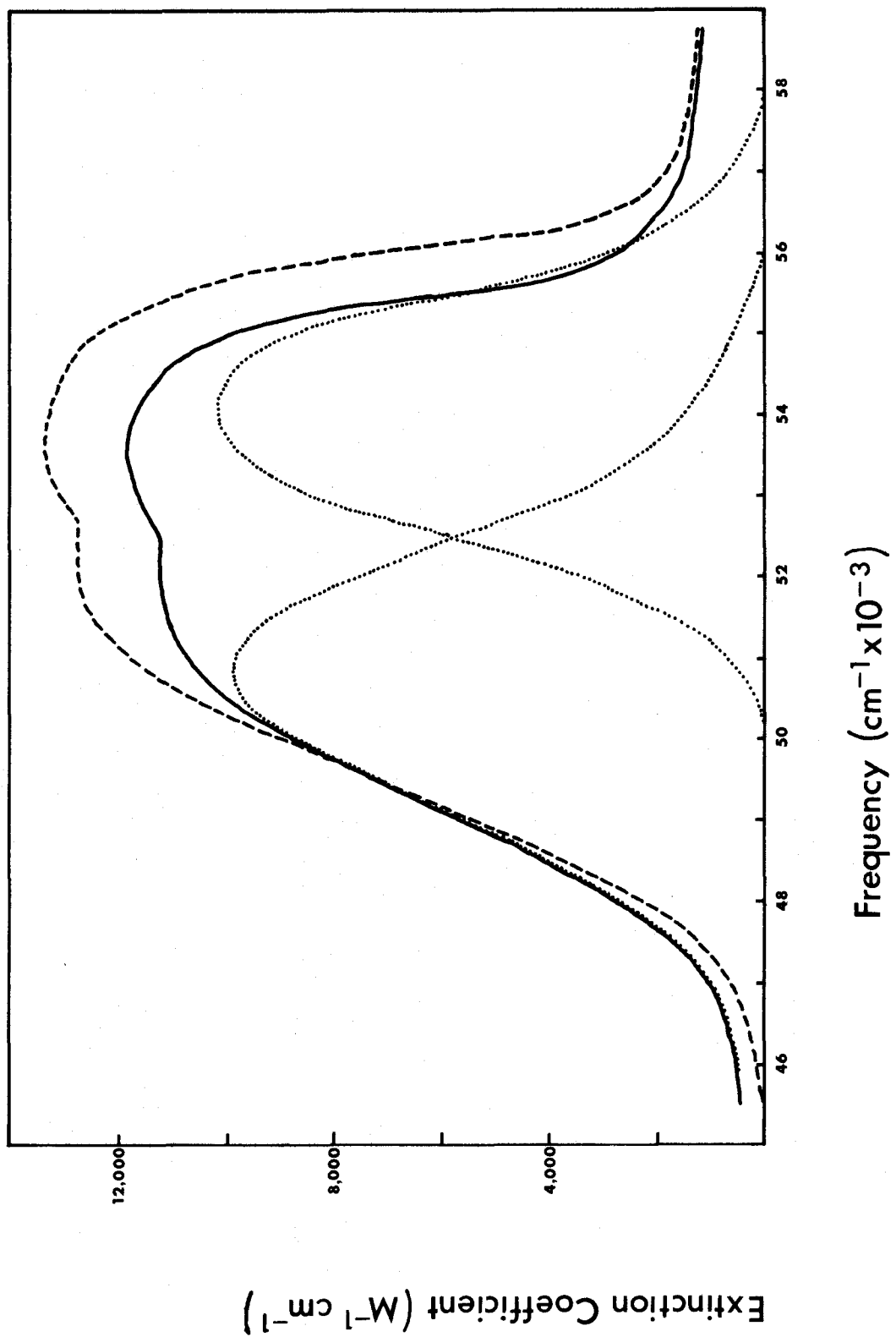


FIGURE 7

Figure 7

Electronic Spectrum of KI

--- Spectrum in  $\text{H}_2\text{O}$

$$c = 2.06 \times 10^{-3} \text{M}$$

$$b = 0.028 \text{ cm}$$

-- Spectrum in  $\text{D}_2\text{O}$

$$c = 2.14 \times 10^{-3} \text{M}$$

$$b = 0.028 \text{ cm}$$

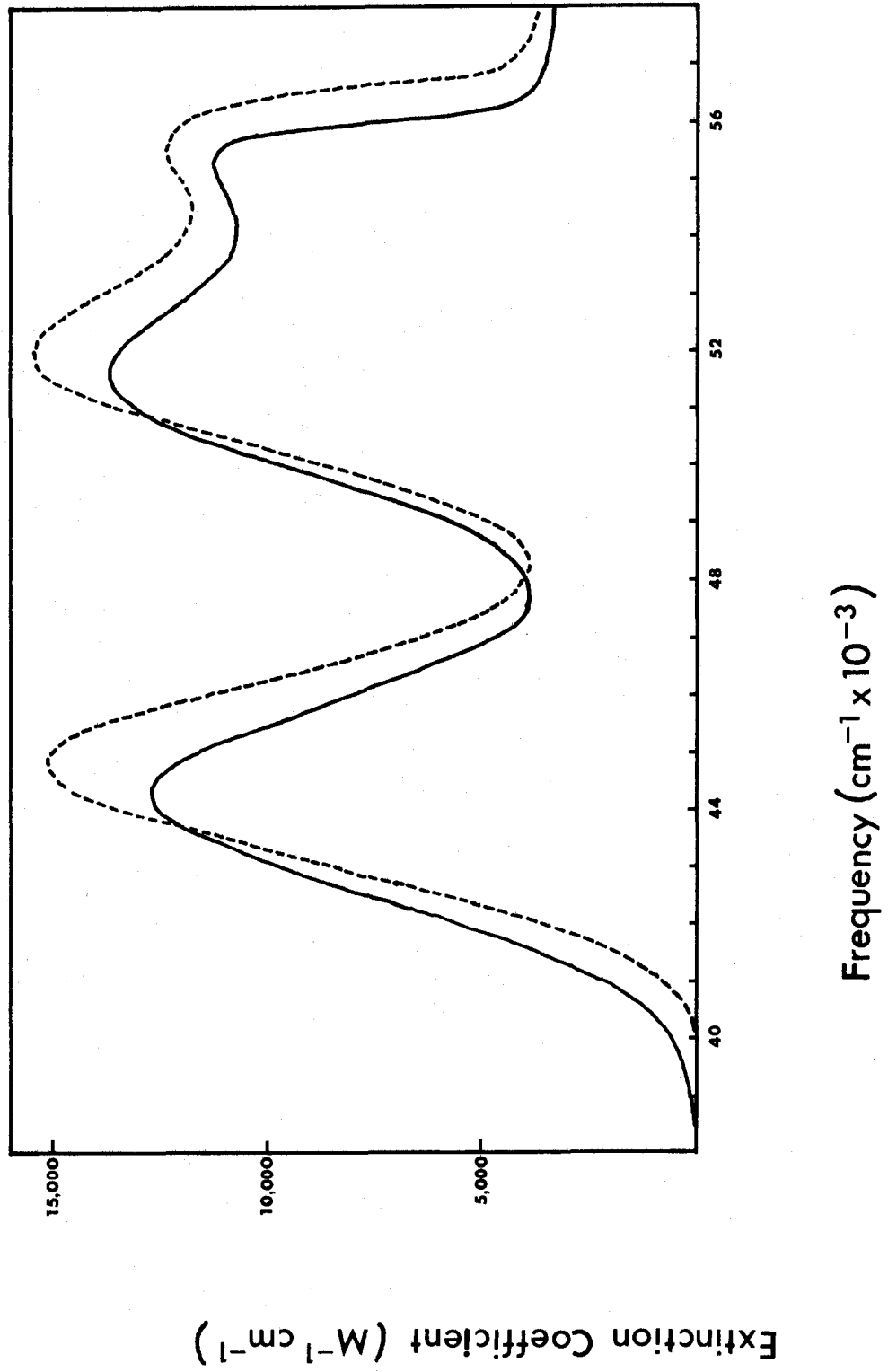


TABLE V

Solution Spectra of  $\text{Cl}^-$ ,  $\text{Br}^-$ ,  $\text{I}^-$ 

	Frequency ( $\text{cm}^{-1}$ )					
	$\text{Cl}^-$		$\text{Br}^-$		$\text{I}^-$	
	$\text{H}_2\text{O}$	$\text{D}_2\text{O}$	$\text{H}_2\text{O}$	$\text{D}_2\text{O}$	$\text{H}_2\text{O}$	$\text{D}_2\text{O}$
$\text{X}^- \rightarrow \text{X}(^2\text{P}_{3/2}) + \text{e}^-_{\text{aq}}$	54,570	55,335	50,800	51,165	44,270	44,750
$\text{X}^- \rightarrow \text{X}(^2\text{P}_{1/2}) + \text{e}^-_{\text{aq}}$	55,595	56,355	54,100	54,605	51,600	52,000
Doublet Splitting	1025	1020	3300	3440	7330	7250
Gas Phase Doublet Splitting <sup>24</sup>	880		3690		7600	
Halide Vapour Doublet Splitting <sup>12</sup>			3300		7200	
Ionization Potential <sup>25</sup> (estimated from gas phase data) ( $\text{kcal mole}^{-1}$ )	$\text{Cl}^-$		$\text{Br}^-$		$\text{I}^-$	
	83.67		77.91		70.99	
( $\text{cm}^{-1}$ )	29,280		27,265		24,845	



Figures 8 and 9 show the electronic spectra of KSCN and KCN respectively. It is beyond the scope of this work to do more than draw attention to the resolved components which appear to correspond to both intra-ligand electronic transitions and CTTS transitions.

None of the simple anions would dissolve in acetonitrile.

FIGURE 8

Figure 8

Electronic Spectrum of KSCN

— Spectrum in  $\text{H}_2\text{O}$

c =  $4.12 \times 10^{-3} \text{M}$

b = 0.028 cm

... Resolved components of spectrum in  $\text{H}_2\text{O}$

--- Spectrum in  $\text{D}_2\text{O}$

b = 0.028 cm

c =  $4.12 \times 10^{-3} \text{M}$

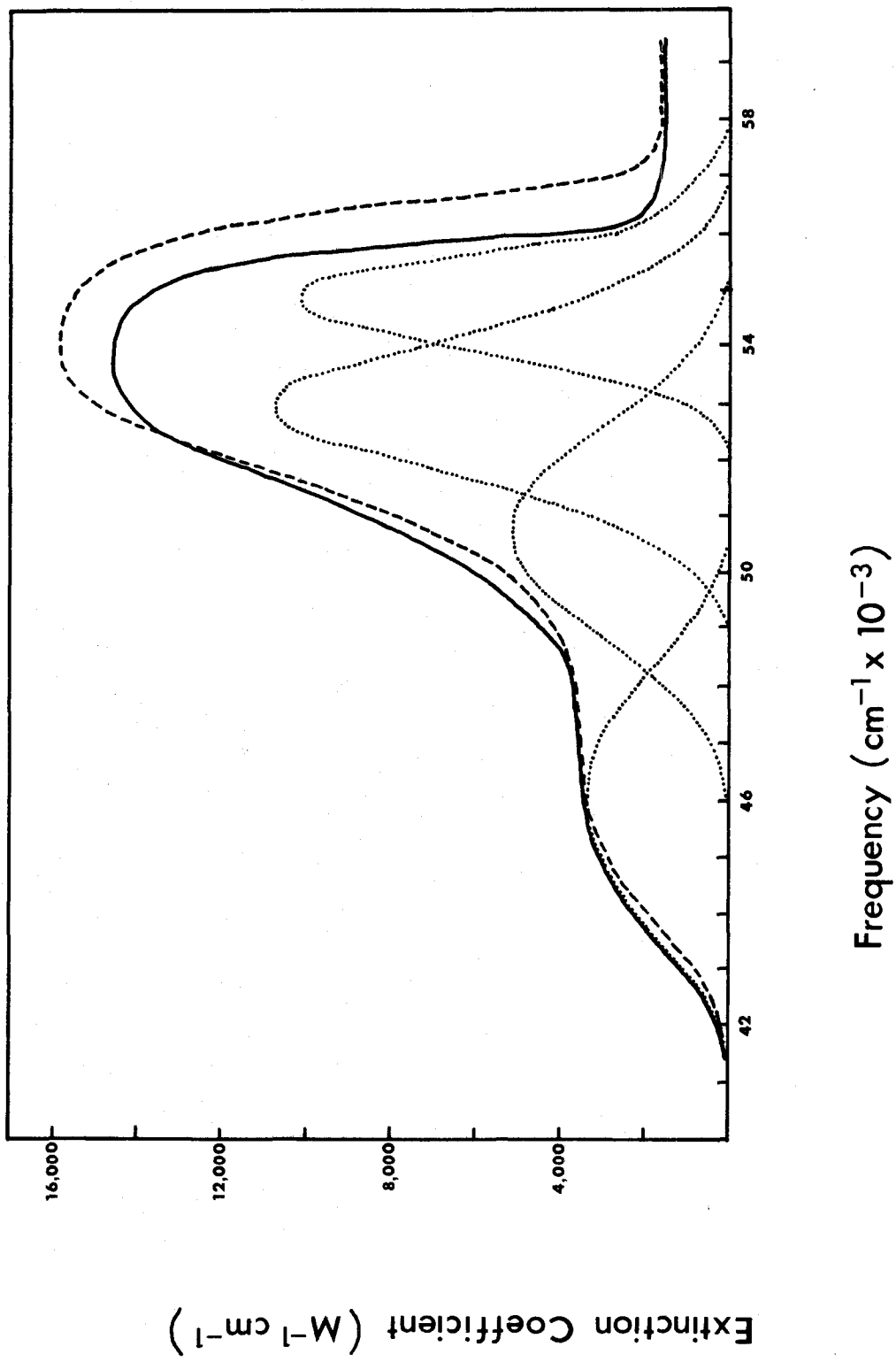


FIGURE 9

Figure 9

Electronic Spectrum of KCN

— Spectrum in  $H_2O$

$$c = 1.05 \times 10^{-2} M$$

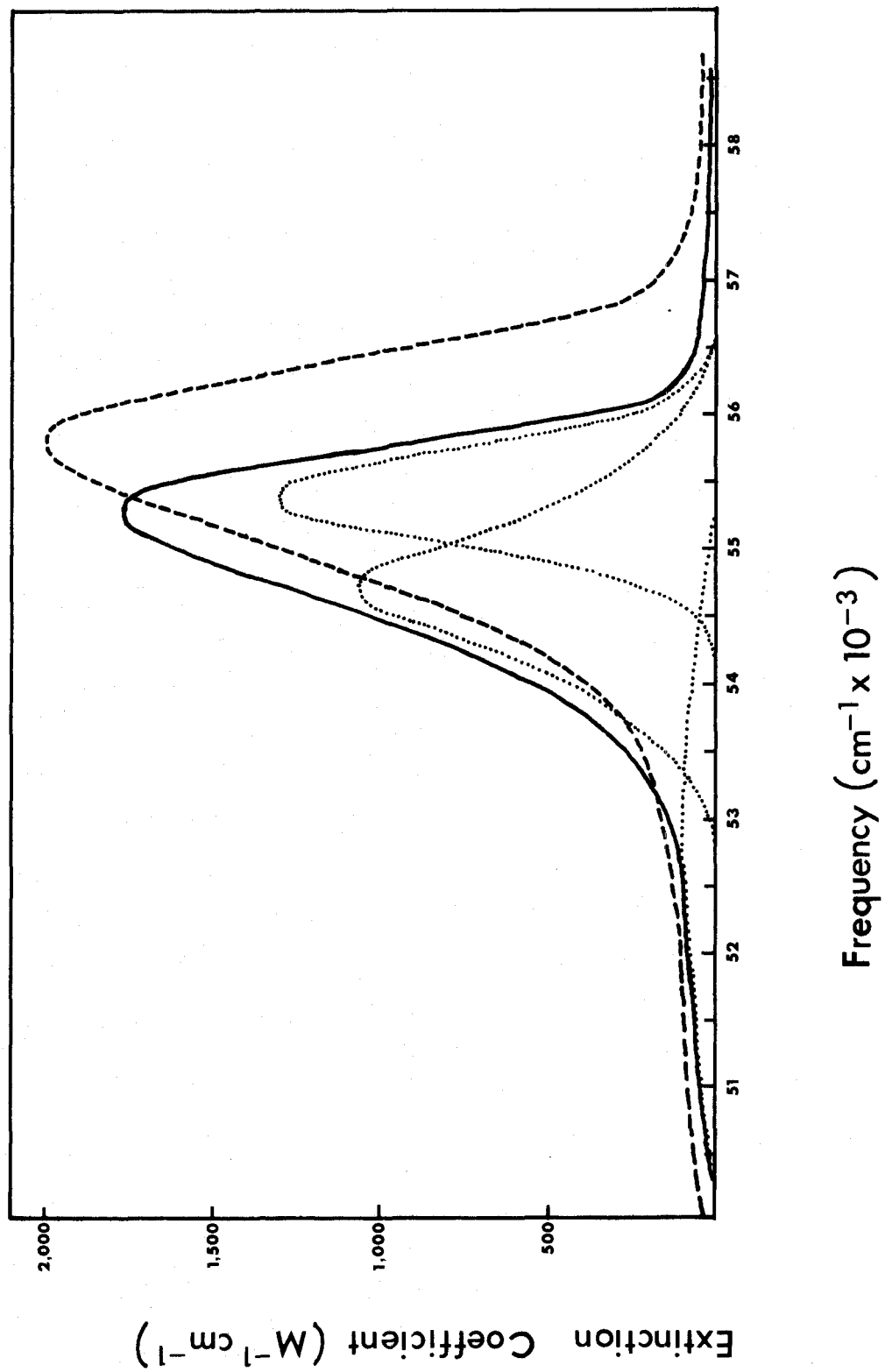
$$b = 0.028 \text{ cm}$$

.. Resolved components of spectrum in  $H_2O$

-- Spectrum in  $D_2O$

$$c = 1.69 \times 10^{-2} M$$

$$b = 0.028 \text{ cm}$$



The solvent effect on the high frequency portion of the spectrum of  $\text{PtCl}_4^{2-}$  is illustrated in Figure 10. Comparison of Figures 11 and 12 shows the effect on a larger part of the spectrum. The hydrolysis tendencies of the other halide complexes prevented similar comparisons from being made. The stability of the cyanide complexes allowed their spectra to be run in water, deuterium oxide, and acetonitrile; however the solvent effects on frequency were substantially reduced.

Figure 13 is typical of the increase in resolution gained by lowering the temperature of the thin film samples. This technique proved to be an invaluable aid in resolving the spectra using Gaussian analysis. Table VI lists the anions and complexes whose spectra were subjected to Gaussian analysis. It is important to take note of the potential of the thin film technique. The thin film technique as applied to studies of the generally intense charge transfer bands is comparable to single crystal studies of the usually weak ligand field bands. The major drawback is that the applicability is restricted by any inherent crystalline properties of the film: the more crystalline the thin film, the lower the resolution.

Tables VII, VIII, and IX summarize the frequencies and assignments for the resolved spectral components of the chloride complexes (Figures 11, 12, 14, 15), the bromide complexes (Figures 16, 17, 18), and the cyanide complexes (Figures 19, 20, 21) respectively. The assignments and their bases are discussed in the next section.

It is to be noted that the chloride and bromide complexes of palladium undergo a change of structure when the potassium counter-ion is replaced with the tetra-n-butylammonium ion. In effect the change from aqueous to non-aqueous solvent forces the square planar  $\text{PdX}_4^{2-}$  to



TABLE VI

## Spectra Subjected to Gaussian Analysis

Species	H <sub>2</sub> O	D <sub>2</sub> O	CH <sub>3</sub> CN
KCl, KBr, KI	x	x	
KCN, KSCN	x	x	
PtCl <sub>4</sub> <sup>2-</sup> b	x	x	x
PtBr <sub>4</sub> <sup>2-</sup> b			x
Pt(CN) <sub>4</sub> <sup>2-</sup> b	x	x	x
Pd <sub>2</sub> Cl <sub>6</sub> <sup>2-</sup> c			x
Pd <sub>2</sub> Br <sub>6</sub> <sup>2-</sup> c			x
Pd(CN) <sub>4</sub> <sup>2-</sup> b	x	x	x
AuCl <sub>4</sub> <sup>1-</sup> c			a
AuBr <sub>4</sub> <sup>1-</sup> c			x
Au(CN) <sub>4</sub> <sup>1-</sup> b			x
Pt(en)Cl <sub>2</sub>	x	x	

a resolution not necessary

b the low temperature thin film spectrum was recorded

c sample crystallized on preparation of thin film

dimerize to  $\text{Pd}_2\text{X}_6^{2-}$  where two of the halide ligands act as bridges.

Figure 10

Figure 10

Solvent Dependence of the High Frequency Electronic  
Spectrum of  $\text{PtCl}_4^{2-}$

- Diagram Y: A Spectrum in  $\text{H}_2\text{O}$   
 $c = 1.08 \times 10^{-3} \text{M}$   
 $b = 0.028 \text{ cm}$
- B Spectrum in  $\text{D}_2\text{O}$   
 $c = 0.964 \times 10^{-3} \text{M}$   
 $b = 0.028 \text{ cm}$
- C Spectrum in  $\text{CH}_3\text{CN}$   
 $c = 2.36 \times 10^{-3} \text{M}$   
 $b = 0.010 \text{ cm}$

Diagram X: Positions of maxima of the resolved components

- A Solvent  $\text{H}_2\text{O}$   
B Solvent  $\text{D}_2\text{O}$   
C Solvent  $\text{CH}_3\text{CN}$

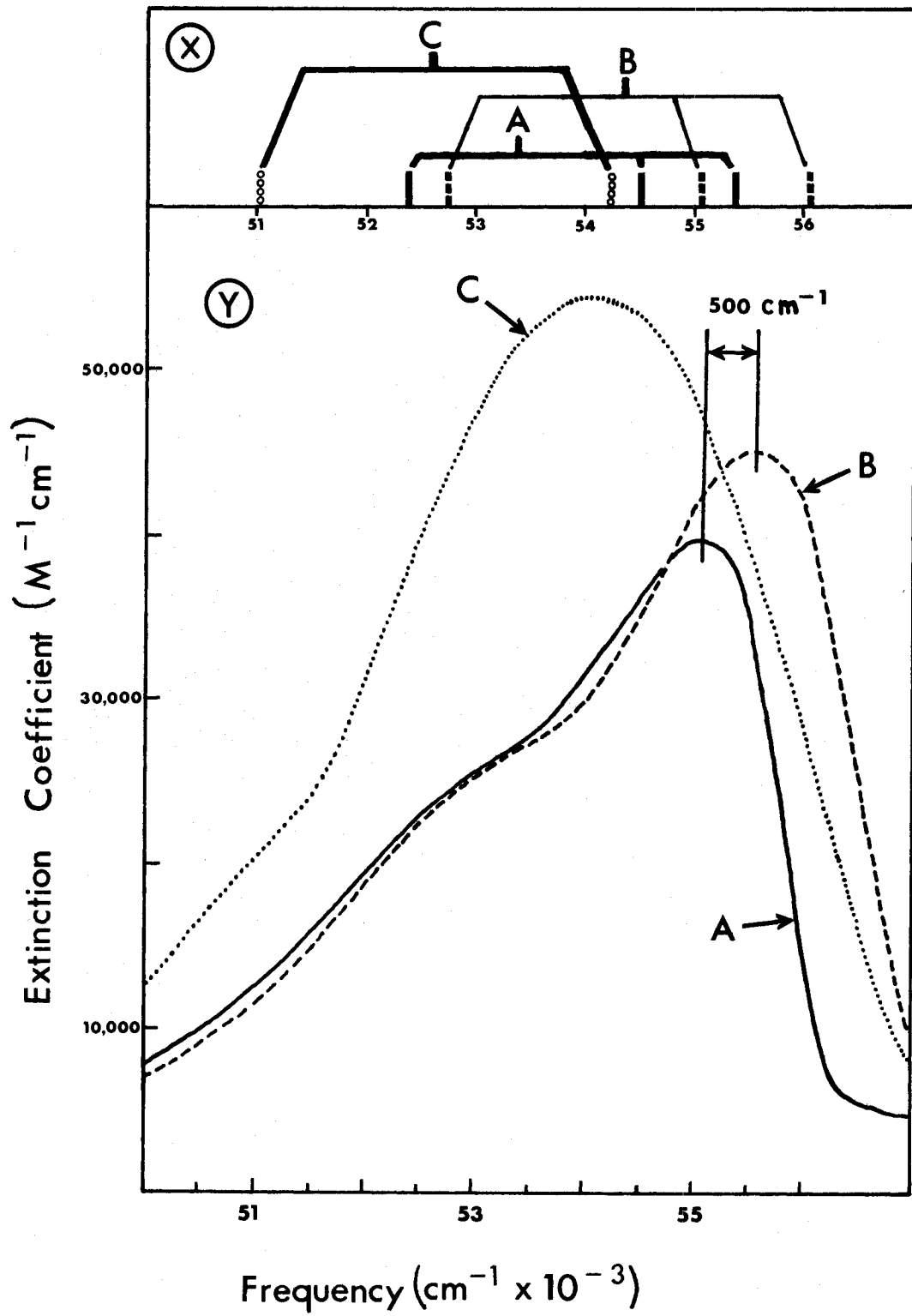


FIGURE 11

Figure 11

Electronic Spectrum of  $\text{PtCl}_4^{2-}$  in  $\text{H}_2\text{O}$

A c =  $2.55 \times 10^{-2} \text{M}$

b = 1.00 cm

B c =  $4.00 \times 10^{-3} \text{M}$

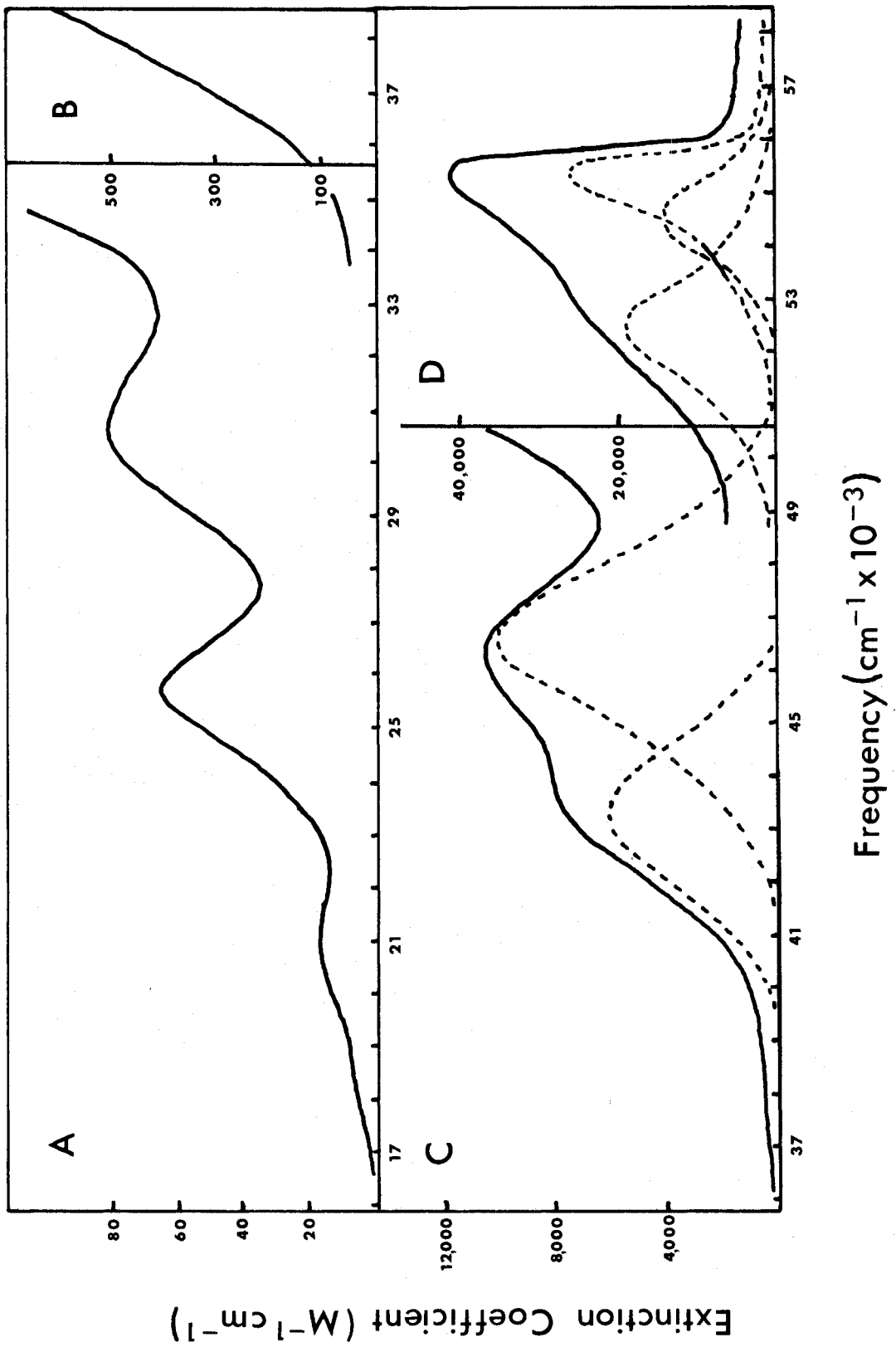
b = 1.00 cm

C c =  $1.04 \times 10^{-4} \text{M}$

b = 1.00 cm

D c =  $1.08 \times 10^{-3} \text{M}$

b = 0.028 cm



Frequency ( $cm^{-1} \times 10^{-3}$ )

Extinction Coefficient ( $M^{-1} cm^{-1}$ )



FIGURE 12

Figure 12

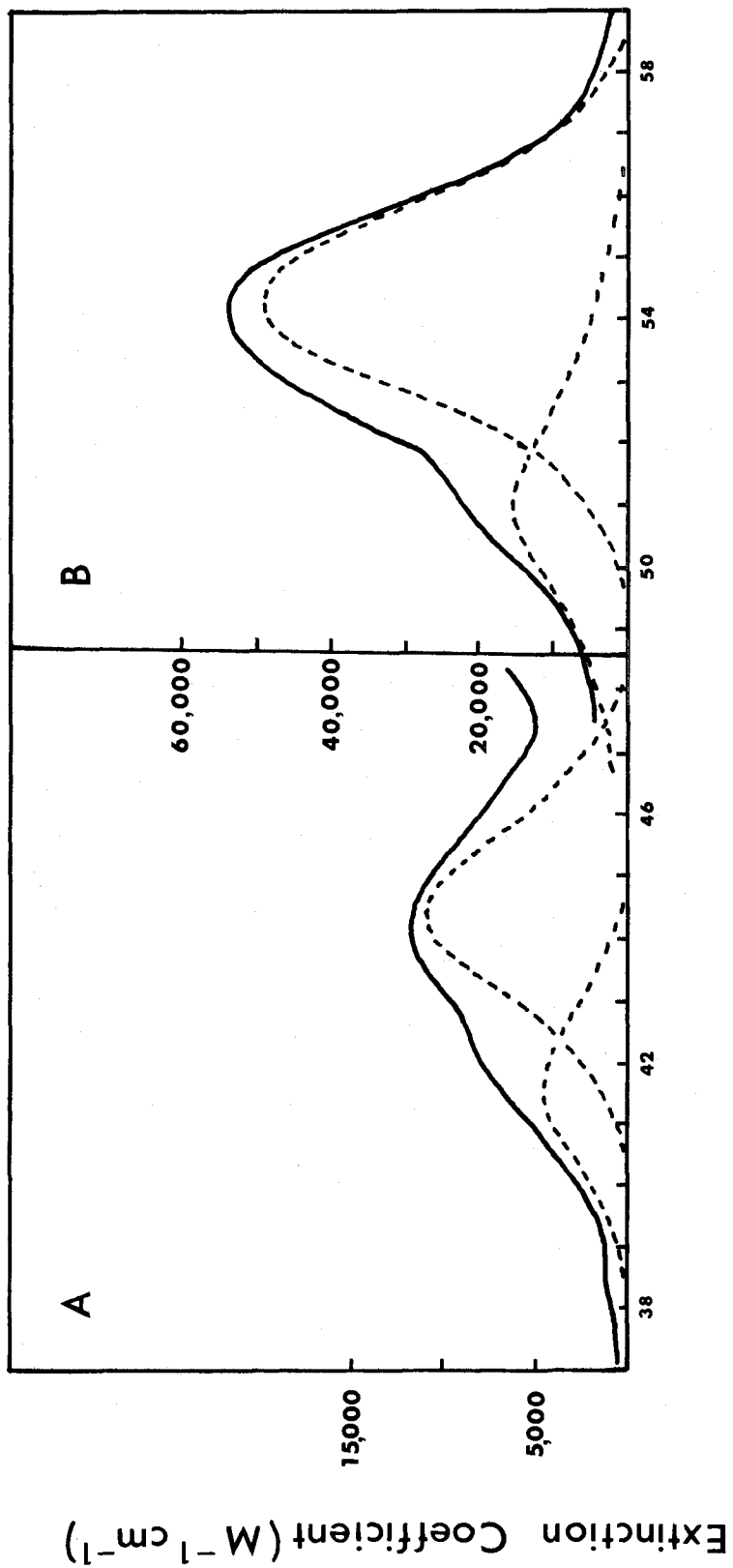
Electronic Spectrum of  $\text{PtCl}_4^{2-}$  in  $\text{CH}_3\text{CN}$

A c =  $6.18 \times 10^{-3}\text{M}$

b = 0.010 cm

B c =  $2.36 \times 10^{-3}\text{M}$

b = 0.010 cm



Frequency ( $cm^{-1} \times 10^{-3}$ )

FIGURE 13

Figure 13

Electronic Spectrum of  $\text{Pd}(\text{CN})_4^{2-}$  :

Thin Film Sample on Quartz Plate

A  $297^\circ\text{K}$

B Tip  $87^\circ\text{K}$

Plate  $168^\circ\text{K}$

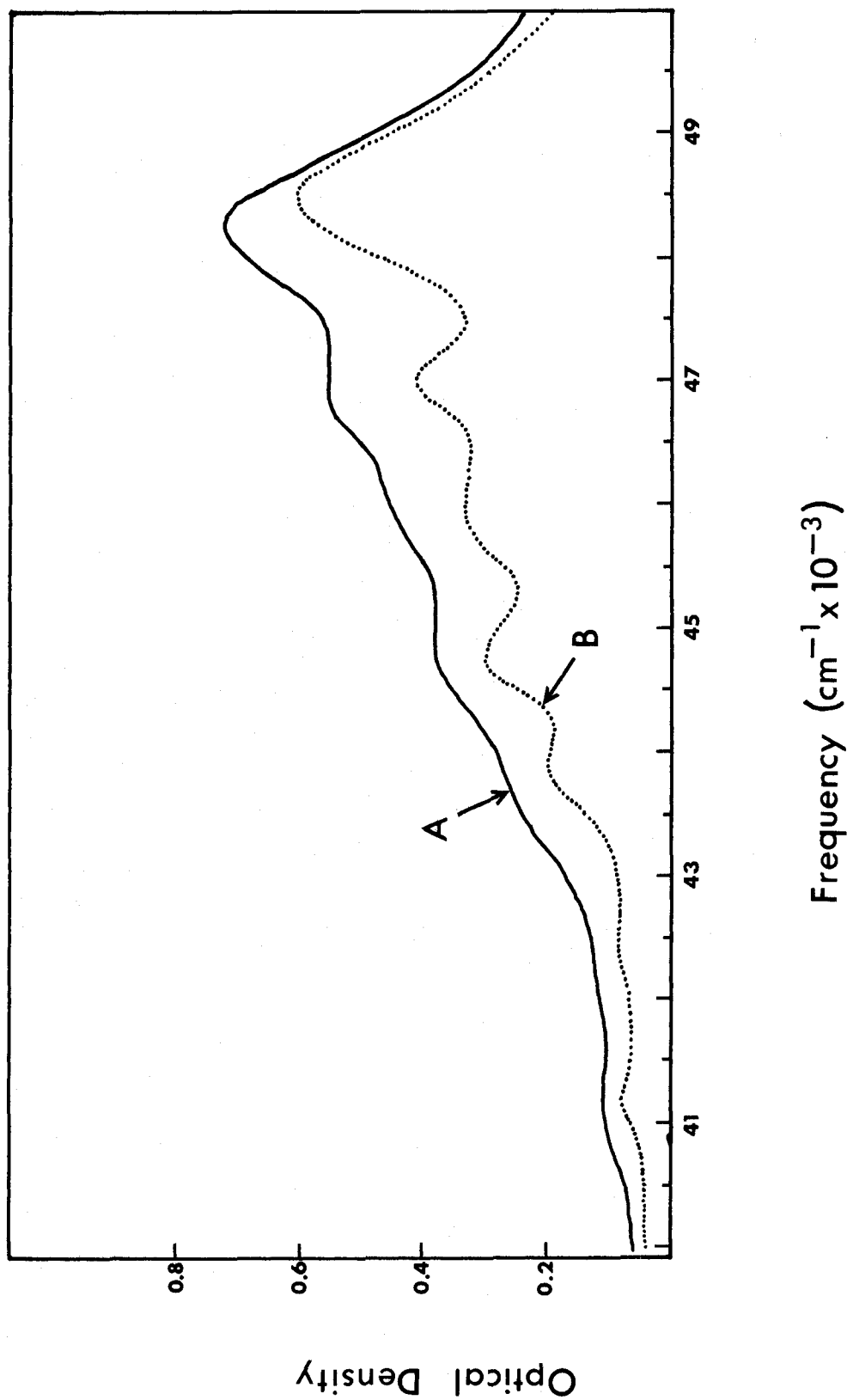


FIGURE 14

Figure 14

Electronic Spectrum of  $\text{Pd}_2\text{Cl}_6^{2-}$  in  $\text{CH}_3\text{CN}$

A c =  $6.0 \times 10^{-3}\text{M}$

b = 0.010 cm

B c =  $1.34 \times 10^{-3}\text{M}$

b = 0.010 cm



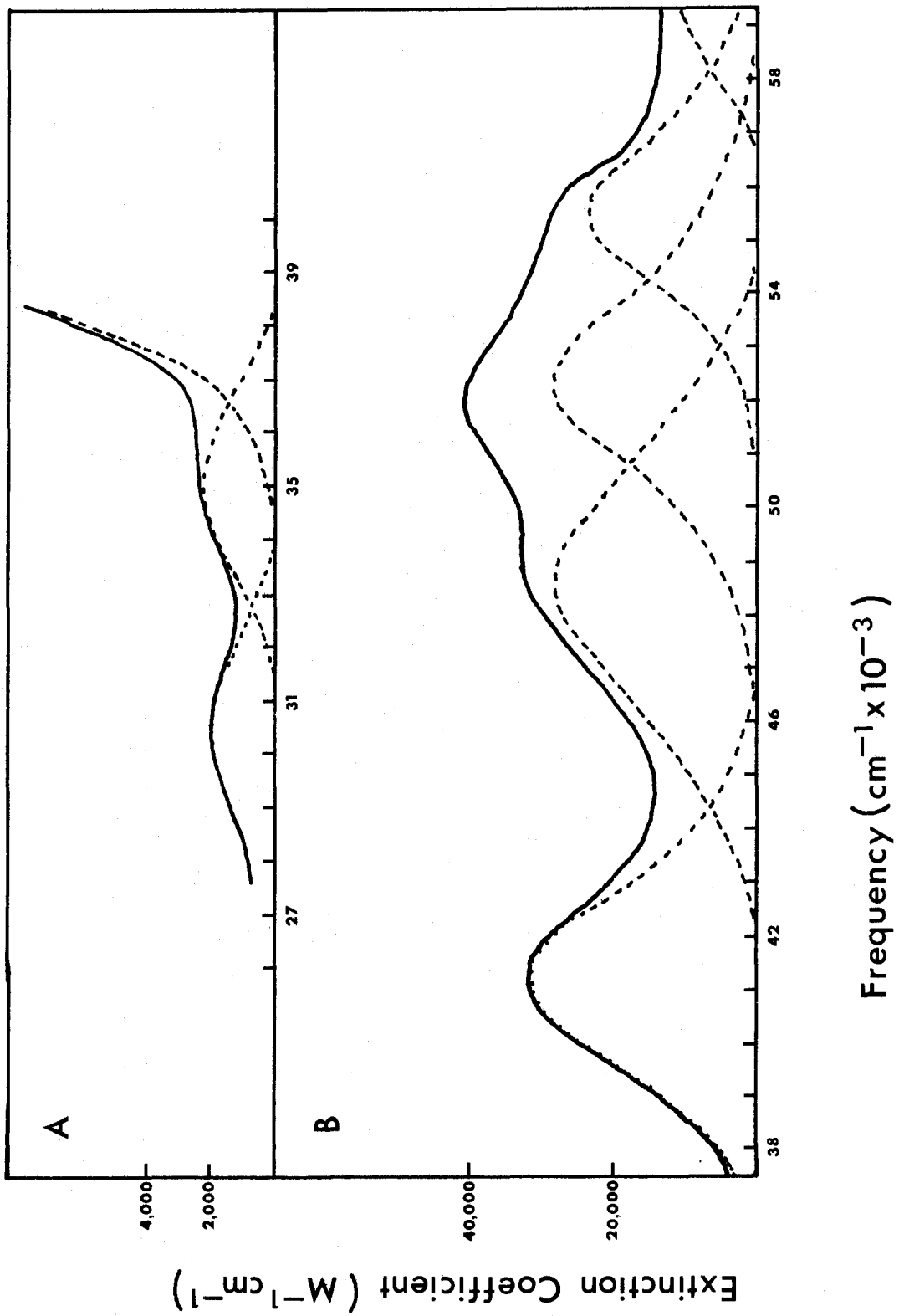


FIGURE 15

Figure 15

Electronic Spectrum of  $\text{AuCl}_4^{1-}$  in  $\text{CH}_3\text{CN}$

$$c = 3.61 \times 10^{-3} \text{ M}$$

$$b = 0.0074 \text{ cm}$$

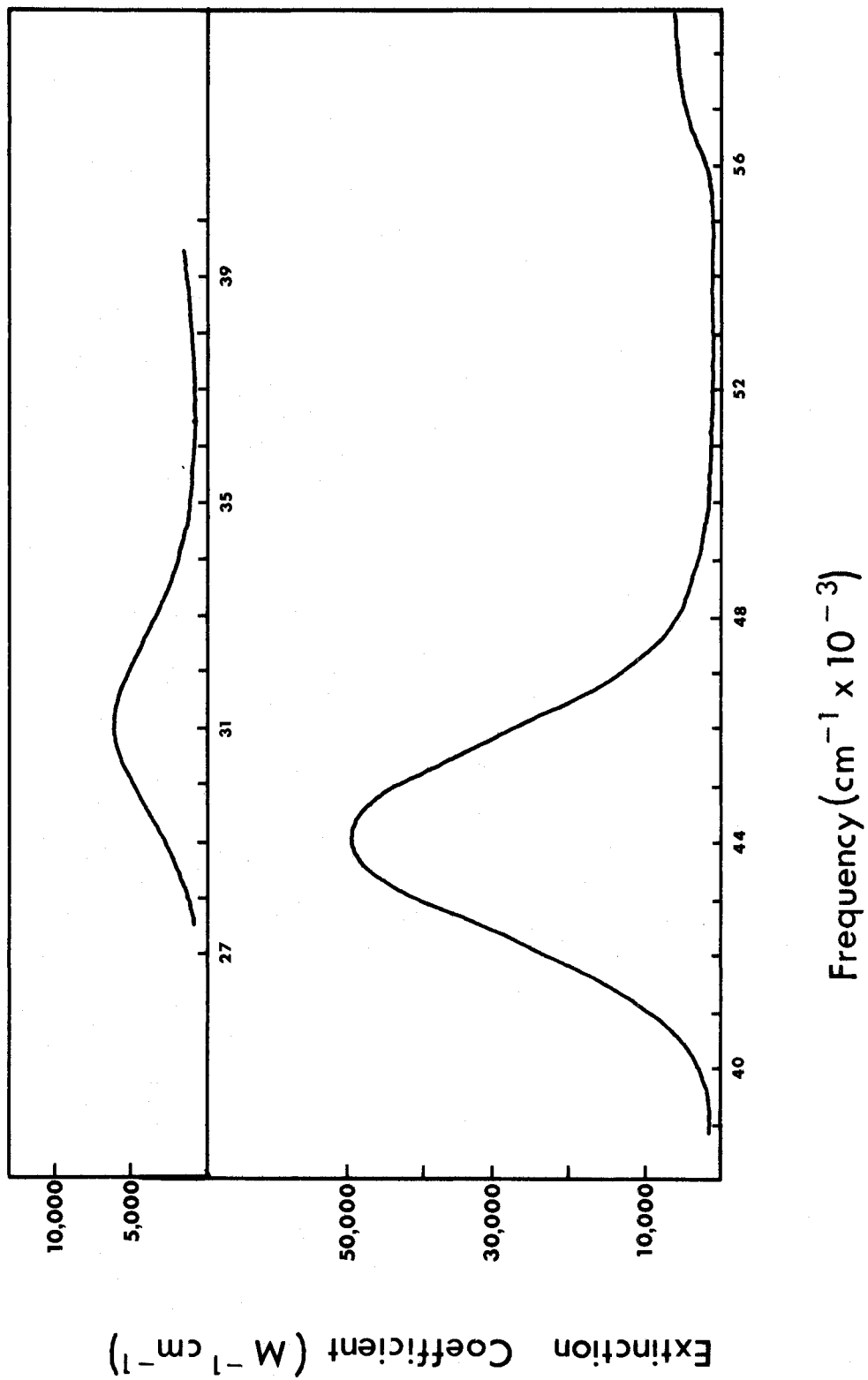


TABLE VII  
Electronic Spectra of Square Planar Chloride Complexes

ORBITAL TRANSITION	TERM TRANSITION	$[\text{PtCl}_4]^{2-} \cdot \text{H}_2\text{O}$	$[\text{PtCl}_4]^{2-} \cdot \text{D}_2\text{O}$	$[\text{PtCl}_4]^{2-} \cdot \text{CH}_3\text{CN}$	$[\text{PdCl}_2]^{2-} \cdot \text{CH}_3\text{CN}$	$[\text{AuCl}_4]^{-} \cdot \text{CH}_3\text{CN}$	Frequency, $\text{cm}^{-1}$ (extinction coefficient, $\text{M}^{-1} \text{cm}^{-1}$ )
$2 b_{2g}^* \rightarrow 2b_{1g}$	${}^1A_{1g} \rightarrow {}^1A_{2g}$	25,740 (63.3) <sup>a</sup>	25,750 (62.0) <sup>a</sup>	24,750 (59.6) <sup>b</sup>	22,200 (350) <sup>b</sup>	21,930 (17.3) <sup>b</sup>	
$2 e_g^* \rightarrow 2b_{1g}$	$\rightarrow E_g$	30,650 (79.1) <sup>a</sup>	30,650 (76.7) <sup>a</sup>	29,500 (66.4) <sup>b</sup>	24,940 (490) <sup>b</sup>	26,520 (319) <sup>b</sup>	
$2 a_{1g}^* \rightarrow 2b_{1g}$	$\rightarrow B_{1g}$	38,000 (500) <sup>a</sup>	38,000 (514) <sup>a</sup>	37,500 (453) <sup>a</sup>			
$1 b_{2u}^{\pi} \rightarrow 2b_{1g}$	$\rightarrow A_{2u}$	43,200 (6173)	43,320 (6415)	41,530 (4100)			30,310 (1935) <sup>B</sup>
$2 e_u^{\pi} \rightarrow 2b_{1g}$	$\rightarrow E_u(1)$	46,470 (10,327)	46,650 (10,231)	44,300 (10,360)			34,980 (2200) <sup>T</sup>
$1 e_u^{\sigma} \rightarrow 2b_{1g}$	$\rightarrow E_u(2)$	52,400 (18,841)	52,740 (20,963)	51,030 (15,100)			41,190 (32,000) <sup>B</sup>
							48,440 (28,100) <sup>T</sup>
$2 b_{2g}^* \rightarrow 2a_{2u}$	$\rightarrow B_{1u}$						
$2 e_g^* \rightarrow 2a_{2u}$	$\rightarrow E_u(3)$	54,520 (13,808)	55,110 (22,222)	54,230 (50,400)	52,210 (28,400)	57,700 (5330) sh	
$2 a_{1g}^* \rightarrow 2a_{2u}$	$\rightarrow A_{2u}$						55,490 (24,000)
$2 b_{2g}^* \rightarrow 3e_u$	$\rightarrow E_u(4)$						
$2 e_g^* \rightarrow 3e_u$	$\rightarrow A_{1u}, A_{2u}$						
	$\rightarrow B_{1u}, B_{2u}$						
$2 a_{1g}^* \rightarrow 3e_u$	$\rightarrow E_u(5)$						

CTTS (tentative)

55,400(4x6,488) 56,200(4x6,463)

a not resolved

b Reference 14.

B Bridge

T Terminal

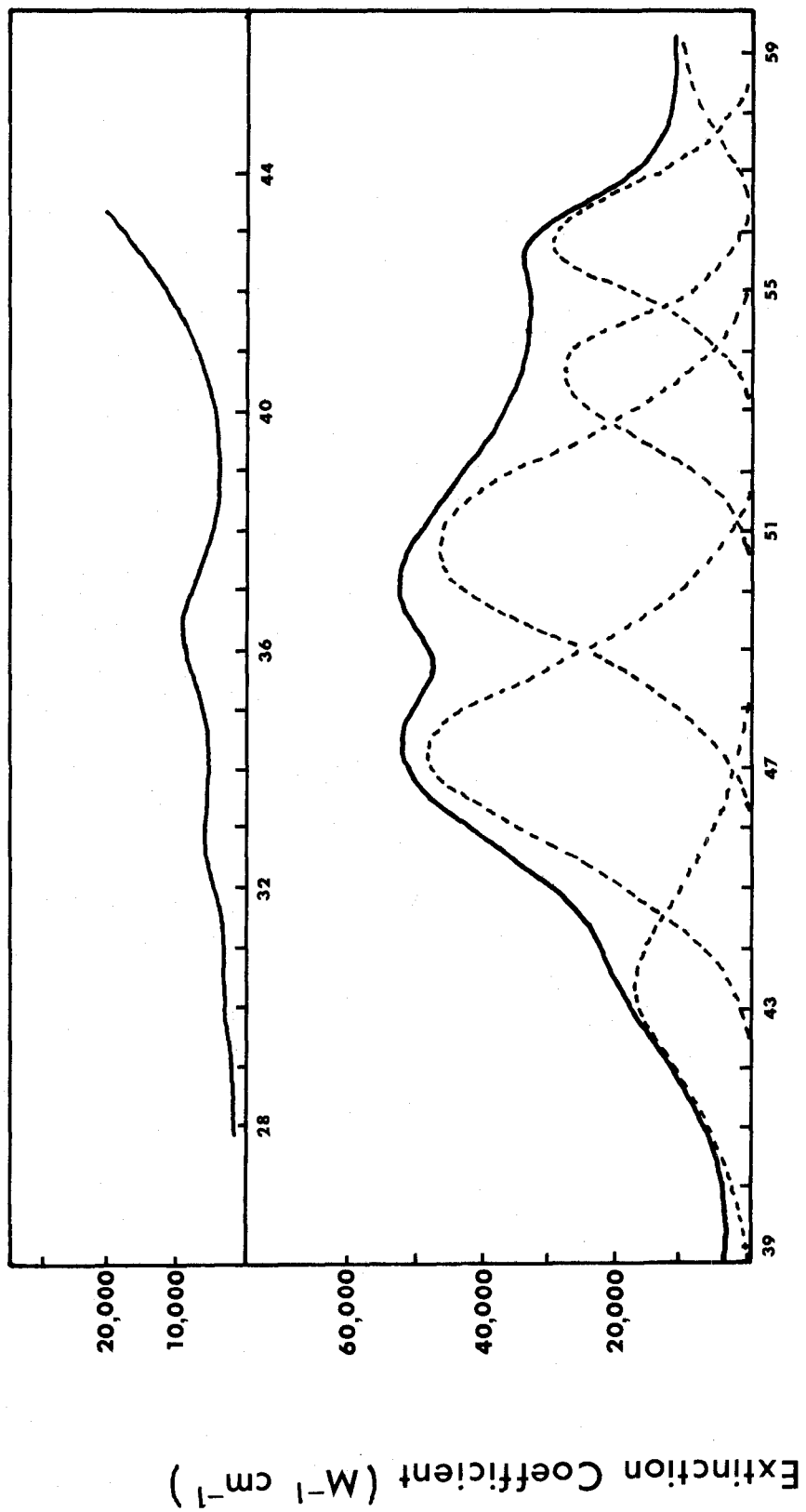
FIGURE 16

Figure 16

Electronic Spectrum of  $\text{PtBr}_4^{2-}$  in  $\text{CH}_3\text{CN}$

$$c = 2.26 \times 10^{-3} \text{ M}$$

$$b = 0.010 \text{ cm}$$



Frequency ( $cm^{-1} \times 10^{-3}$ )



FIGURE 17

Figure 17

Electronic Spectrum of  $\text{Pd}_2\text{Br}_6^{2-}$  in  $\text{CH}_3\text{CN}$

A c =  $6.08 \times 10^{-3} \text{ M}$

b = 0.010 cm

B c =  $1.615 \times 10^{-3} \text{ M}$

b = 0.010 cm

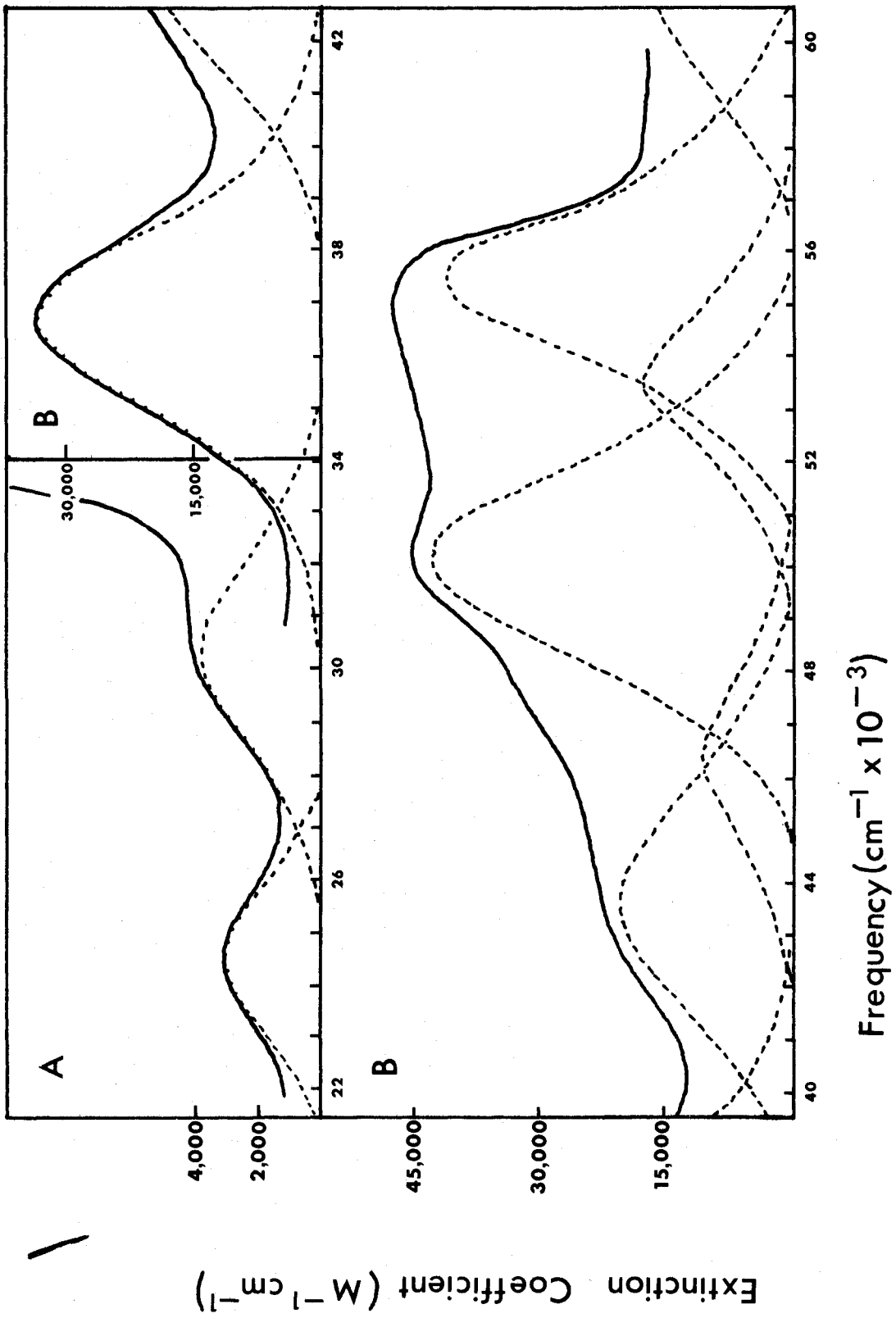


Figure 18

FIGURE 18

Electronic Spectrum of  $\text{AuBr}_4^{1-}$  in  $\text{CH}_3\text{CN}$

$$c = 4.13 \times 10^{-3} \text{M}$$

$$b = 0.0074 \text{ cm}$$

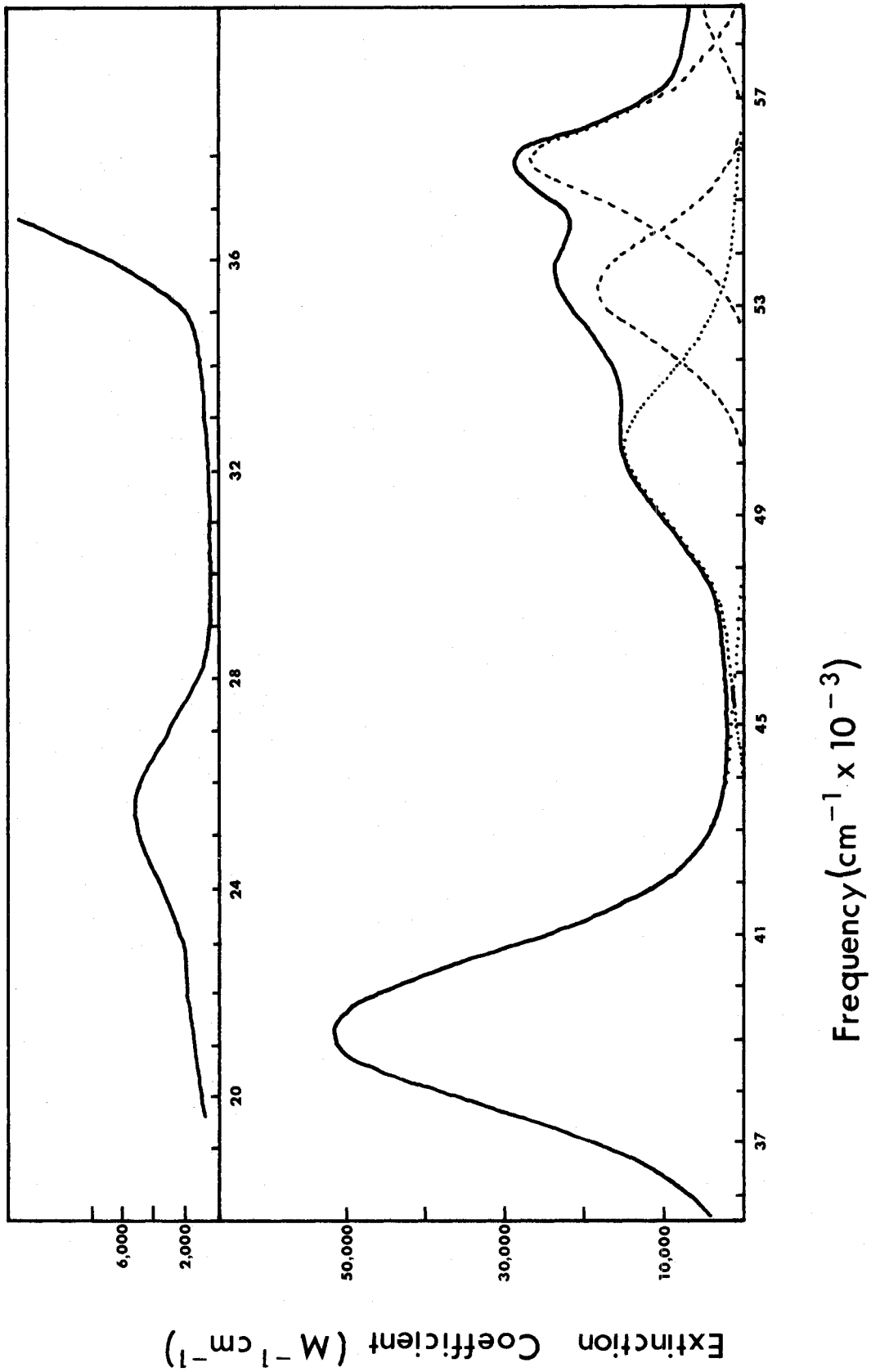


TABLE VIII

Electronic Spectra of Square Planar Bromide Complexes  
 Frequency,  $\text{cm}^{-1}$  (Extinction coefficient,  $\text{M}^{-1} \text{cm}^{-1}$ )

ORBITAL TRANSITION	TERM TRANSITION	$[\text{PtBr}_4]^{2-}$ $-\text{CH}_3\text{CN}$	$[\text{Pd}_2\text{Br}_6]^{2-}$ $-\text{CH}_3\text{CN}$	$[\text{AuBr}_4]^{-}$ $-\text{CH}_3\text{CN}$
$2 b_{2g}^* + 2b_{1g}^*$	$1A_{1g} + 1A_{2g}$	23,150 (1.26) <sup>b</sup>	16,950 (74.8) <sup>b</sup>	18,500 (119) <sup>b</sup>
$2 e_g^* + 2b_{1g}^*$	$+ E_g$	26,880 (187) <sup>b</sup>	19,420 (481) <sup>b</sup>	21,320 (1090) <sup>a</sup>
$2 a_{1g}^* + 2b_{1g}^*$	$+ B_{1g}$	30,100 (2100) <sup>a</sup>		
$1 b_{2u}^n \rightarrow 2b_{1g}^*$	$\rightarrow A_{2u}$	33,300 (4790) <sup>a</sup>	$\left. \begin{array}{l} 24,520 (3010) \\ 30,330 (3910) \end{array} \right\} \begin{array}{l} B \\ T \end{array}$	25,400 (4775) <sup>a</sup>
$2 e_u^n \rightarrow 2b_{1g}^*$	$\rightarrow E_u (1)$	36,100 (8600) <sup>a</sup>		
$1 e_u^b \rightarrow 2b_{1g}^*$	$\rightarrow E_u (2)$	43,350 (16,800)	$\left. \begin{array}{l} 36,710 (33,100) \\ 43,590 (20,100) \end{array} \right\} \begin{array}{l} B \\ T \end{array}$	39,150 (48,625)
$2 b_{2g}^* + 2a_{2u}^*$	$+ B_{1u}$			
$2 e_g^* \rightarrow 2a_{2u}^*$	$\rightarrow E_u (3)$	47,210 (48,300)	46,300 (10,550)	50,300 (14,000)
$2 a_{1g}^* \rightarrow 2a_{2u}^*$	$\rightarrow A_{2u}$	50,740 (46,600)	50,120 (42,300)	53,330 (17,700)
$2 b_{2g}^* \rightarrow 3e_u^*$	$\rightarrow E_u (4)$	53,620 (27,900)	53,470 (16,750)	55,800 (26,725)
$2e_g^* \rightarrow 3e_u^*$	$\begin{array}{l} A_{1u}, A_{2u}, \\ \rightarrow B_{1u}, B_{2u} \end{array}$			
$2a_{1g}^* \rightarrow 3e_u^*$	$\rightarrow E_u (5)$	55,870 (30,200)	55,470 (38,400)	

a not resolved      B Bridge

b Reference 14.      T Terminal

FIGURE 19



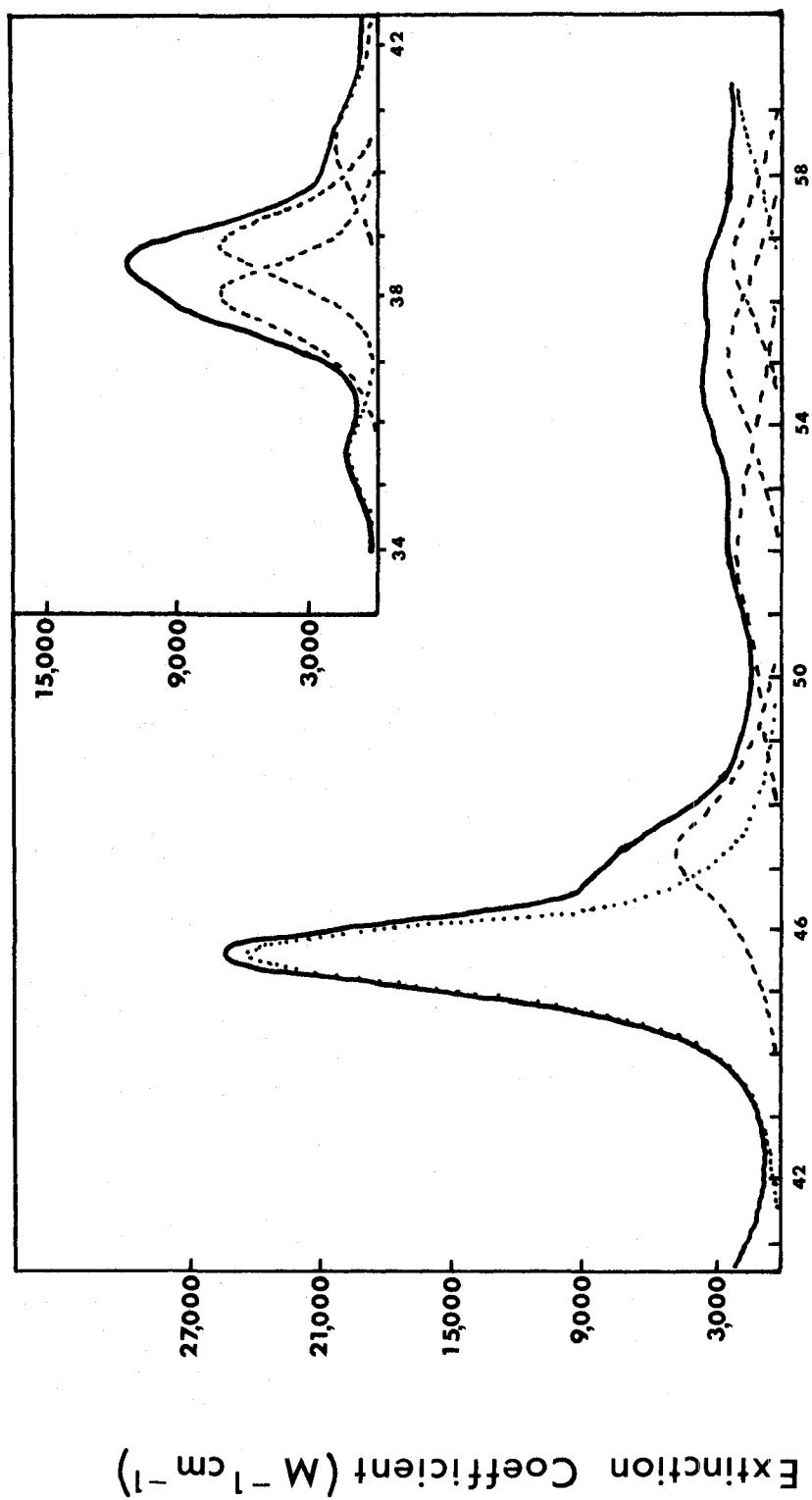
FIGURE 19

Electronic Spectrum of  $\text{Pt}(\text{CN})_4^{2-}$  in  $\text{CH}_3\text{CN}$

$$c = 6.94 \times 10^{-3} \text{ M}$$

$$b = 0.010 \text{ cm}$$

19-1111



Frequency ( $\text{cm}^{-1} \times 10^{-3}$ )

Extinction Coefficient ( $\text{M}^{-1} \text{cm}^{-1}$ )

FIGURE 20

FIGURE 20

Electronic Spectrum of  $\text{Pd}(\text{CN})_4^{2-}$  in  $\text{CH}_3\text{CN}$

$c = 8.03 \times 10^{-3} \text{M}$

$b = 0.0074 \text{ cm}$

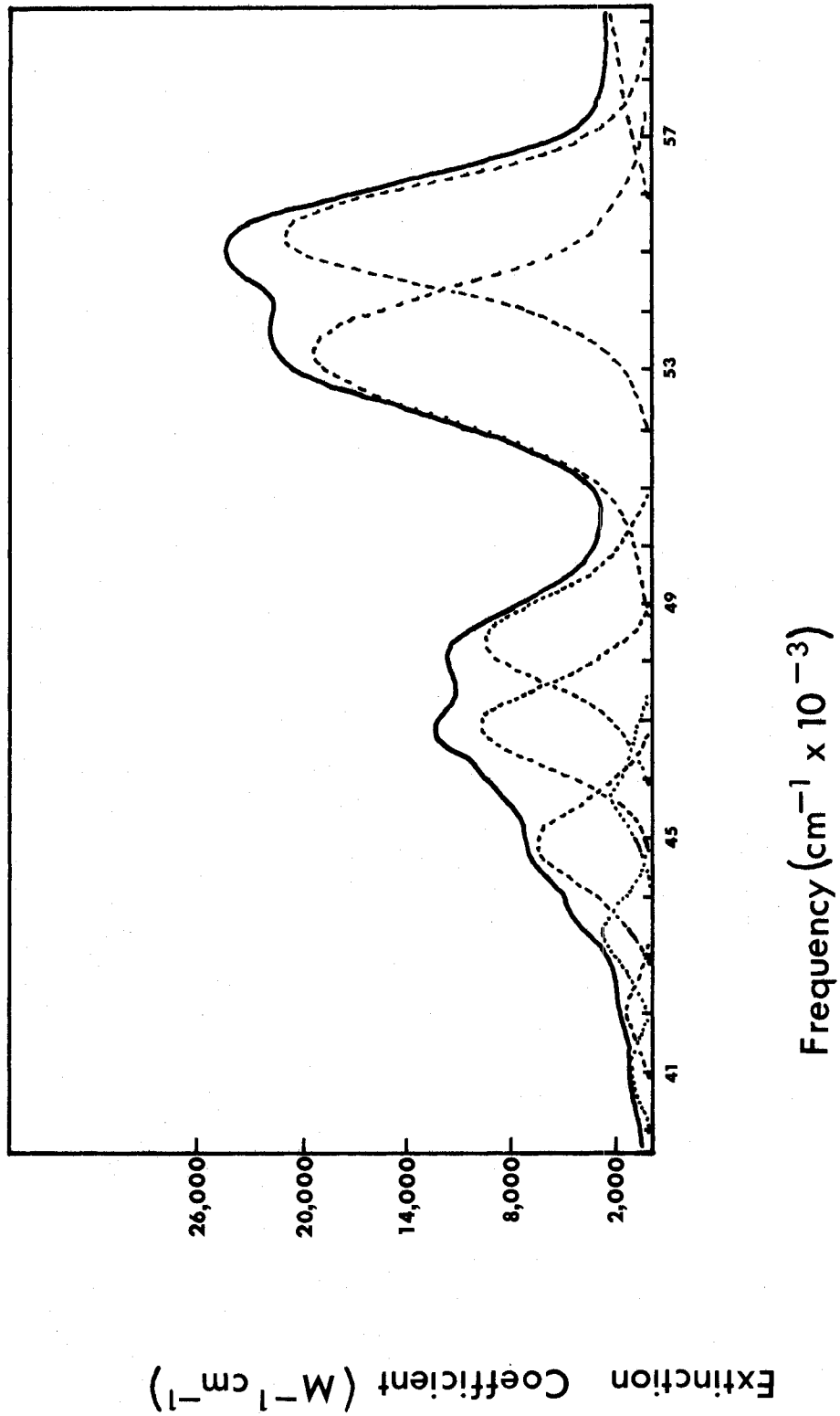


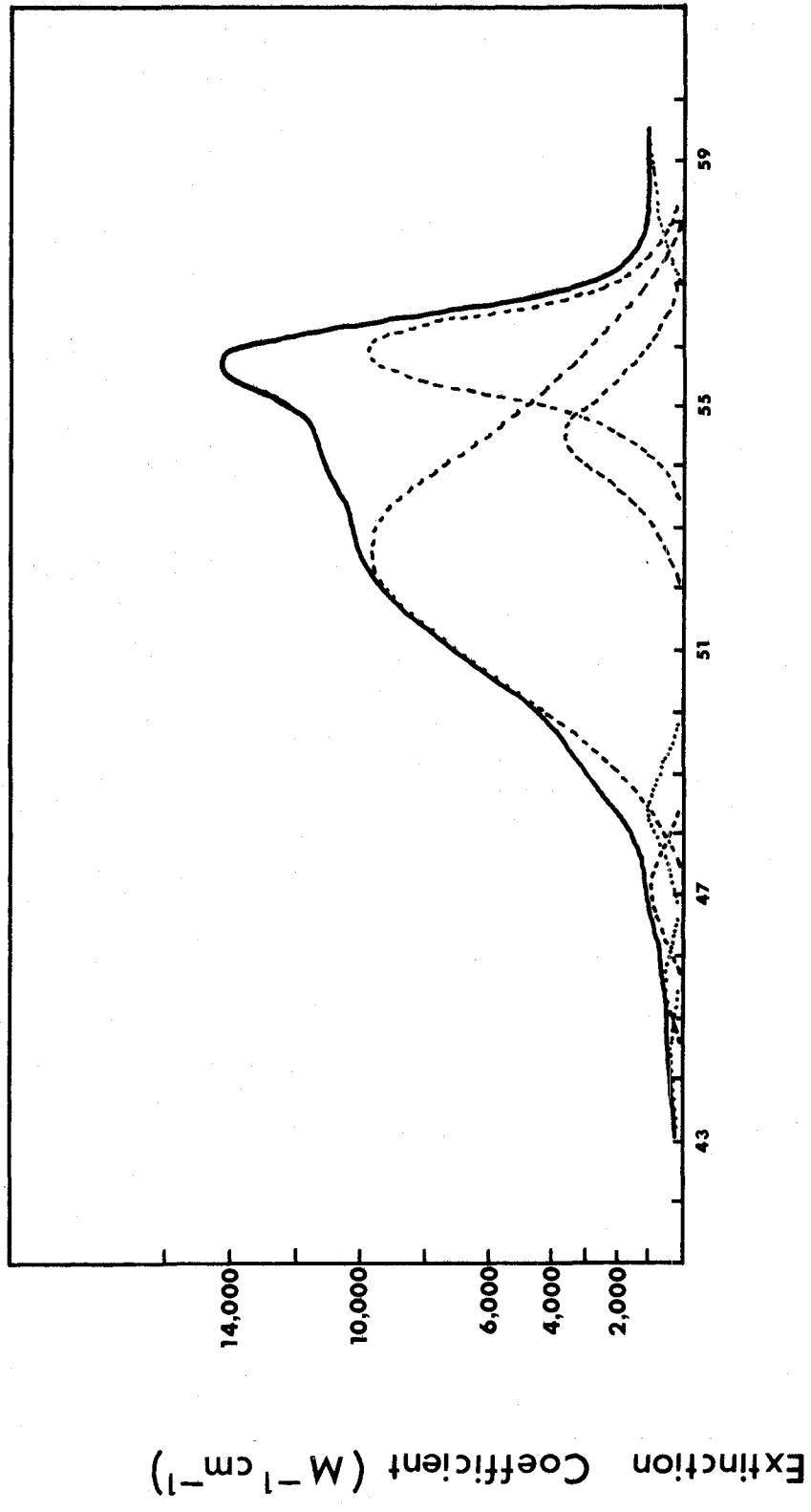
FIGURE 21

Figure 21

Electronic Spectrum of  $\text{Au}(\text{CN})_4^{1-}$  in  $\text{CH}_3\text{CN}$

$$c = 7.16 \times 10^{-3} \text{M}$$

$$b = 0.0074 \text{ cm}$$



Frequency ( $cm^{-1} \times 10^{-3}$ )



TABLE IX

## Electronic Spectra of Square Planar Cyanide Complexes

ORBITAL TRANSITION		TERM TRANSITION	$[\text{Pt}(\text{CN})_4]_{\text{H}_2\text{O}}$	$[\text{Pt}(\text{CN})_4]_{\text{D}_2\text{O}}$	$[\text{Pt}(\text{CN})_4]_{\text{CH}_3\text{CN}}$
$2 b_{2g}^* + 2 b_{1g}^*$	$1 A_{1g} + 1 A_{2g}$		broad asym. peak MAX. (55,900 (3620))	broad asym. peak MAX. (56,250 (3460))	52,230 (1880)
$2 e_g^* + 2 b_{1g}^*$	$1 E_g$				54,980 (2450)
$2 a_{1g}^* + 2 b_{1g}^*$	$1 B_{1g}$				56,720 (2100)
$2 b_{2g}^* + 2 a_{2u}^*$	$1 B_{1u}$		35,860 (1601)	35,860 (1535)	35,470 (1140)
$2 e_g^* \rightarrow 2 a_{2u}^*$	$1 E_u$ (3)		38,600 (6380)	38,600 (6220)	38,050 (7120)
$2 a_{1g}^* \rightarrow 2 a_{2u}^*$	$1 A_{2u}$		39,540 (7830)	39,540 (7720)	38,820 (7070)
$2 b_{2g}^* \rightarrow 3 e_u^*$	$1 E_u$ (4)		41,480 (1530)	41,480 (1720)	40,540 (1560)
$2 e_g^* \rightarrow 3 e_u^*$	$1 A_{2u}, 1 B_{2u}, 1 B_{1u}, 1 B_{2u}$		46,350 (20,100)	46,360 (20,200)	45,540 (24,600)
$2 a_{1g}^* \rightarrow 3 e_u^*$	$1 E_u$ (5)		47,960 (4660)	47,960 (4690)	47,220 (4790)

Frequency,  $\text{cm}^{-1}$  (Extinction coefficient,  $\text{M}^{-1}\text{cm}^{-1}$ )

$[\text{Pt}(\text{CN})_4]_{\text{H}_2\text{O}}$

$[\text{Pt}(\text{CN})_4]_{\text{D}_2\text{O}}$

$[\text{Pt}(\text{CN})_4]_{\text{CH}_3\text{CN}}$

broad asym.  
peak  
MAX.  
(55,900 (3620))

broad asym.  
peak  
MAX.  
(56,250 (3460))

$1 A_{2u}$  (4)

$1 A_{2u}, 1 B_{2u}, 1 B_{1u}, 1 B_{2u}$

$1 E_u$  (5)

TABLE IX (continued)

Electronic Spectra of Square Planar Cyanide Complexes

Frequency,  $\text{cm}^{-1}$  (Extinction coefficient,  $\text{M}^{-1}\text{cm}^{-1}$ )

ORBITAL TRANSITION	TERM TRANSITION	$[\text{Pd}(\text{CN})_4]_{\text{H}_2\text{O}}^{2-}$	$[\text{Pd}(\text{CN})_4]_{\text{D}_2\text{O}}^{2-}$	$[\text{Pd}(\text{CN})_4]_{\text{CH}_3\text{CN}}^{2-}$	$[\text{Au}(\text{CN})_4]_{\text{CH}_3\text{CN}}^{1-}$
$2b_{2g}^* + 2b_{1g}^*$	${}^1A_{1g} + {}^1A_{2g}$	41,660 (992)	41,660 (969)	41,000 (1077)	44,500 (321)
$2e_g^* + 2b_{1g}^*$	${}^1E_g$	43,910 (1825)	43,910 (1690)	43,340 (2730)	45,630 (472)
$2a_{1g}^* + 2b_{1g}^*$	${}^1B_{1g}$	46,070 (1825)	46,070 (1530)	45,760 (2155)	47,000 (944)
$2b_{2g}^* + 2a_{2u}^*$	${}^1B_{1u}$	42,800 (800)	42,800 (844)	42,000 (1380)	48,360 (1000)
$2e_g^* \rightarrow 2a_{2u}^*$	$\rightarrow {}^1E_u$ (3)	45,260 (6180)	45,280 (5720)	44,870 (6640)	52,630 (9810)
$2a_{1g}^* \rightarrow 2a_{2u}^*$	$\rightarrow {}^1A_{2u}$	47,190 (6910)	47,190 (6470)	46,870 (9830)	54,530 (3620)
$2b_{2g}^* \rightarrow 3e_u^*$	$\rightarrow {}^1E_u$ (4)	49,180 (10,650)	49,200 (10,150)	48,400 (10,030)	55,870 (9720)
$2e_g^* \rightarrow 3e_u^*$	$\rightarrow \begin{matrix} A_{1u}, A_{2u} \\ B_{1u}, B_{2u} \end{matrix}$	53,980 (15,500)	54,300 (15,750)	53,170 (19,300)	-----
$2a_{1g}^* \rightarrow 3e_u^*$	$\rightarrow {}^1E_u$ (5)	55,570 (19,800)	56,100 (17,900)	55,300 (21,000)	-----

Another complex, dichloroethylenediamineplatinum (II), was examined because it was expected to have a combination of the spectral properties of  $\text{Pt}(\text{NH}_3)_4^{2+}$ , where  $M \rightarrow L$  charge transfer is energetically more accessible than  $L \rightarrow M$  charge transfer, and  $\text{PtCl}_4^{2-}$  where  $L \rightarrow M$  charge transfer is at lower energies. The molecular orbital diagram for this  $C_{2v}$  complex can be seen in Figure 22. The spectrum of dichloroethylenediamineplatinum (II) (Figure 23) was run in water and deuterium oxide; unfortunately the complex was insoluble in acetonitrile. The assignments for the resolved components of the observed band structure can be seen in Table X.

Figure 22

Molecular Orbital Diagram  
 $C_{2v}$

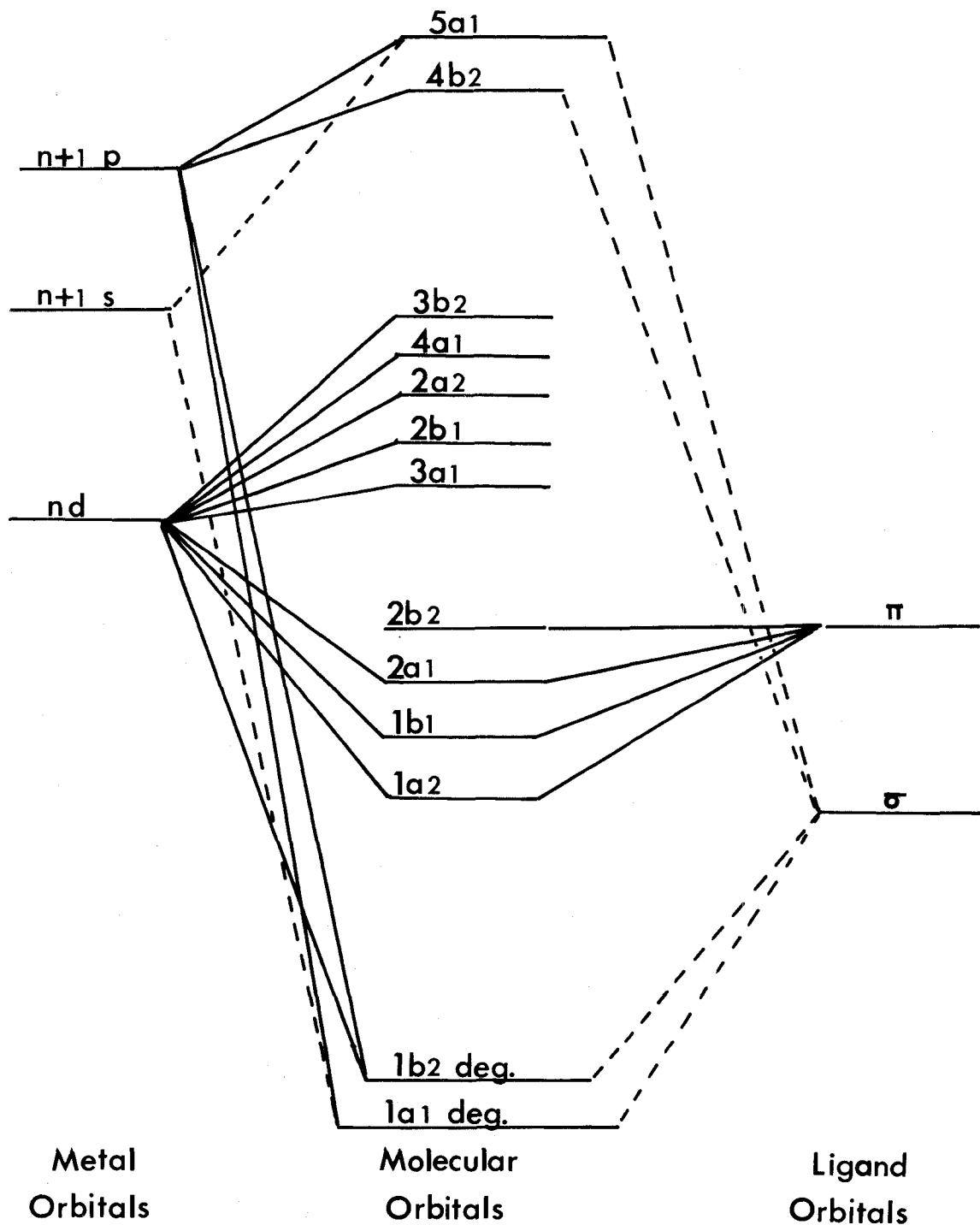


FIGURE 23

Figure 23

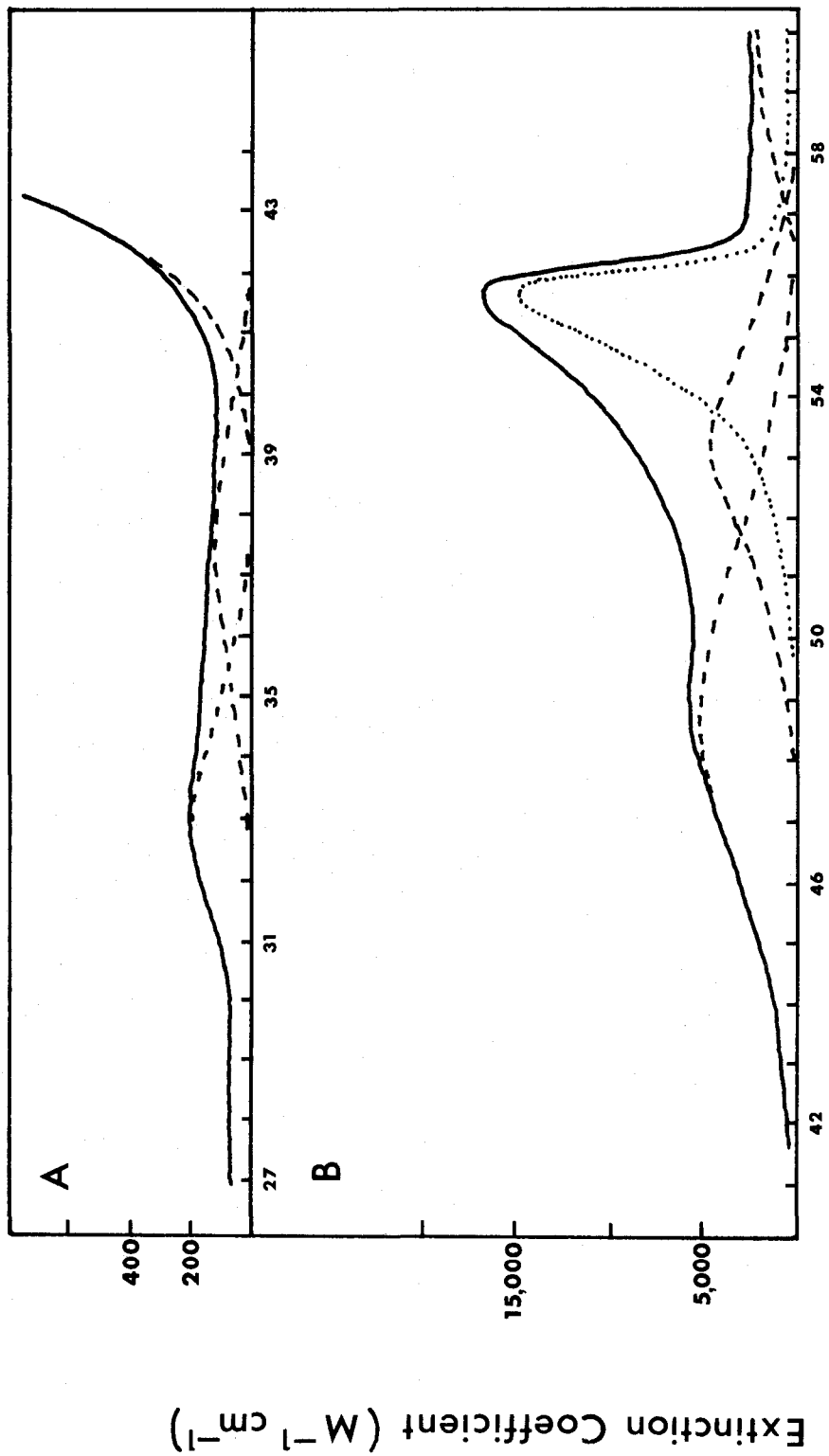
Electronic Spectrum of  $\text{Pt}(\text{en})\text{Cl}_2$  in  $\text{H}_2\text{O}$

A c =  $1.14 \times 10^{-3} \text{M}$

b = 0.4375 cm

B c =  $1.10 \times 10^{-3} \text{M}$

b = 0.028 cm



Frequency ( $\text{cm}^{-1} \times 10^{-3}$ )



TABLE X

Electronic Spectrum of Pt(en)Cl<sub>2</sub>Frequency, cm<sup>-1</sup> (Extinction coefficient, M<sup>-1</sup>cm<sup>-1</sup>)

Orbital Transition	Term Transition	[Pt(en)Cl <sub>2</sub> ·H <sub>2</sub> O]	[Pt(en)Cl <sub>2</sub> ·D <sub>2</sub> O]	
d-d	$\left\{ \begin{array}{l} 4a_1^* \rightarrow 3b_2^* \\ 2a_2^* \rightarrow 3b_2^* \\ 2b_1^* + 3b_2^* \\ 3a_1^* \rightarrow 3b_2^* \end{array} \right.$	${}^1A_1 \rightarrow {}^1B_2$	32,920(181)	32,930(192)
		$\rightarrow {}^1B_1$	37,260(104)	37,260(127)
		$+ {}^1A_2$		
		$\rightarrow {}^1B_2$		
CTTM	$\left\{ \begin{array}{l} 2b_2(\pi^n) \rightarrow 3b_2^* \\ 2a_1 \rightarrow 3b_2^* \\ 1b_1 + 3b_2^* \\ 1a_2 \rightarrow 3b_2^* \end{array} \right.$	$\rightarrow {}^1A_1$	48,390(5260)	48,700(5330)
		$\rightarrow {}^1B_2$		
		$+ {}^1A_2$		
		$\rightarrow {}^1B_1$		
d-p	$\left\{ \begin{array}{l} 4a_1^* \rightarrow 4b_2^* \\ 2a_2^* \rightarrow 4b_2^* \\ 2b_1^* + 4b_2^* \\ 3a_1^* \rightarrow 4b_2^* \end{array} \right.$	$\rightarrow {}^1B_2$	53,030(4580)	53,490(4760)
		$\rightarrow {}^1B_1$		
		$+ {}^1A_2$		
		$\rightarrow {}^1B_2$		
CTTS (tentative)			55,700(2x7400)	56,540(2x6900)

## DISCUSSION

The primary basis which is employed for making our assignments is internal consistency. This approach is required for at least two reasons. The first is the lack of a rigorous theoretical basis. The exact wavefunction describing a complex ion in its ground state would be tremendously complicated. Any attempt to construct such a wavefunction yields only a very approximate result because of the difficulties in evaluating the interelectronic repulsions. Description of excited states is further complicated by the doubt as to exactly which excited state is under consideration; the criterion of minimum energy is no longer useful. A second problem with excited states is the difficulty in estimating the effect of crystal field perturbations. Another complication arises when the symmetry of the excited state is different from that of the ground state. Finally, the theoretical approach takes no account of solvent perturbations; there is no mention of the mixing of solvent orbitals with those of the complex. The second reason for turning to internal consistency is the fact that the techniques normally available for assignments of ligand field bands are not generally operative in the U.V. where most charge transfer bands are observed. Examples are temperature studies to analyze the vibronically-allowed transitions, polarized spectra to examine dichroism in single crystals, and magnetic circular dichroism to detect degenerate states. Thus new criteria such as intensity effects and frequency trends are sought within an internally consistent model for charge transfer bands.

Using the molecular orbital diagrams shown in Figures 1, 2, and 22, the allowed transitions (See Tables II, III, and X) can be determined using

the relationship:

$$\Gamma_g \Gamma_{op} \Gamma_{ex} = \Gamma_t$$

where  $\Gamma_g$  = term representation for the ground state,

$\Gamma_{ex}$  = term representation for the excited state,

$\Gamma_{op}$  = term representation for the electric dipole operator component in the particular symmetry Group of the complex,

and  $\Gamma_t$  = direct product representation. The electronic transition is allowed if the direct product representation ( $\Gamma_{total}$ ) contains the totally symmetric representation ( $\Gamma_1$ ) for the particular symmetry Group. As illustrated before, this selection rule gives rise to the Laporte rule and the spin conservation rule.

Strictly speaking the ligand field bands are forbidden by the Laporte rule since they are essentially d-d in character; however these transitions have finite intensity. In short the Laporte selection rule ( $g \leftrightarrow u, g \leftrightarrow g, u \leftrightarrow u$ ) is relaxed by a partial breakdown of the Born-Oppenheimer Principle<sup>12,26,15,6</sup>. In this event there is a mixing of the molecular electronic and vibrational wave functions (i.e. vibronic coupling). Asymmetric vibrations remove the inversion centre and permit mixing of the symmetric and asymmetric wave functions. Consider as an example the  $'b_{2g}^* \rightarrow 'b_{1g}^*$  ( $'A_{1g} \rightarrow 'A_{2g}$ ) transition in  $PtCl_4^{2-}$ . The electric dipole operator in  $D_{4h}$  symmetry transforms as  $A_{2u} + E_u$ . Evaluating the direct products yields:

$$A_{1g} \otimes A_{2u} \otimes A_{2g} = A_{1u}$$

$$A_{1g} \otimes E_u \otimes A_{2g} = E_u$$

The symmetries of the normal vibrational modes of  $\text{PtCl}_4^{2-}$  are:  $A_{1g}$ ,  $A_{2u}$ ,  $B_{2g}$ ,  $B_{2u}$ ,  $B_{1g}$ , and  $2E_u$ <sup>27, 6</sup>. Thus while the pure electronic transition  $A_{1g} \rightarrow A_{2g}$  is forbidden, the simultaneous excitation of a vibration of  $E_u$  symmetry will make it allowed.

In addition to vibronic coupling, relaxation of the Laporte rule can be achieved through d-p mixing in the ground state and distortions in the excited state. The d-p mixing through the anti-bonding ligand  $\pi^*$  orbitals enhances the ligand field intensities (without especially requiring a vibronic interaction); this same mechanism causes the loss of definite u and g character. Whilst the ground state belongs to the  $D_{4h}$  symmetry Group, the excited states may undergo a distortion approaching Td and under this symmetry strong d-p mixing may be anticipated. An interesting example of a symmetry change upon proceeding from the ground state to the excited state is the photochemical behaviour of  $\text{Pt}(\text{gly})_2$ <sup>5</sup> where radio-isotope labelling has shown the cis  $\rightarrow$  trans photoisomerization to take place by an intramolecular twisting mechanism.

The singlet  $\rightarrow$  triplet ligand field transitions are forbidden not only by Laporte's rule but also by the spin conservation rule. Accordingly their intensities would be even less than the intensities of the singlet  $\rightarrow$  singlet ligand field transitions. Such transitions are in fact observed because spin-orbit coupling mixes the singlet and triplet states<sup>6</sup>.

Consider the  $\pi^n \rightarrow d^*$  charge transfer transitions  $b_{2u}(\pi^n) \rightarrow (b_{1g}^*(\sigma^*))$  and  $e_u(\pi^n) \rightarrow b_{1g}^*(\sigma^*)$ . Any mixing of the non-bonding p(u) orbitals with the s(g) orbitals would give some g character to the  $\pi^n$  levels. This would result in a reduced absorption intensity compared to

that of the  $e_u(\sigma^b) \rightarrow b_{1g}^*(\sigma^*)$  transition. In  $\text{Pt Br}_4^{2-}$  for example, the intensity of the  $b_{2u}(\pi^n) \rightarrow b_{1g}^*$  transition is roughly 30% of the  $e_u(\sigma^b) \rightarrow b_{1g}^*$  absorption intensity.

In the cyanide complexes, the stronger the  $\pi$  covalent bonding, the greater is the mixing of the  $b_{2g}^*$  and  $e_g^*$  levels with the  $a_{2u}^*$  and  $e_u^*$  levels. This interaction could give u character to the  $b_{2g}^*$  and  $e_g^*$  levels with resulting increased intensity in the d-d transitions. The  $e_g^* \rightarrow b_{1g}^*$  transition in  $\text{Pd}(\text{CN})_4^{2-}$  (extinction coefficient  $2730 \text{ M}^{-1} \text{ cm}^{-1}$ ) is much more intense than the same transition in  $\text{Pd}_2\text{Cl}_6^{2-}$  (extinction coefficient  $490 \text{ M}^{-1} \text{ cm}^{-1}$ ). On the other hand this same phenomenon would give g character to the  $a_{2u}^*$  and  $e_u^*$  levels causing decreased intensity in the M  $\rightarrow$  L charge transfer transitions. This is illustrated by comparison of the  $e_g^* \rightarrow a_{2u}^*$  transition intensity of  $\text{Pt}(\text{CN})_4^{2-}$  (extinction coefficient  $7120 \text{ M}^{-1} \text{ cm}^{-1}$  ( $\text{CH}_3\text{CN}$ )) with that of  $\text{PtCl}_4^{2-}$  ( $\epsilon = 50,400 \text{ M}^{-1} \text{ cm}^{-1}$  ( $\text{CH}_3\text{CN}$ )).

Examination of the  $b_{2g}^* \rightarrow a_{2u}^*$  ( ${}^1A_{1g} \rightarrow {}^1B_{1u}$ ) transition shows that it is orbitally forbidden:

$$A_{1g} \otimes A_{2u} \otimes B_{1u} = B_{2g}$$

$$A_{1g} \otimes E_u \otimes B_{1u} = E_g$$

From before<sup>27,6</sup>, the symmetries of the normal vibrational modes of  $\text{PtX}_4^{2-}$  are  $A_{1g}$ ,  $A_{2u}$ ,  $B_{2g}$ ,  $B_{2u}$ ,  $B_{1g}$  and  $2E_u$ . Thus while the pure electronic transition  ${}^1A_{1g} \rightarrow {}^1B_{1u}$  is forbidden, the simultaneous excitation of a vibration of  $B_{2g}$  symmetry will make it allowed. The  $b_{2g}^* \rightarrow a_{2u}^*$  transition intensity of  $\text{Pd}(\text{CN})_4^{2-}$  serves as an example (extinction coefficient  $800 \text{ M}^{-1} \text{ cm}^{-1}$  ( $\text{H}_2\text{O}$ )).

If solvent perturbation is the same in the excited state as in

the ground state then the solvent effect on transition frequency is expected to be small. It is only when solvent perturbation is different in the ground and excited states that a change of solvent is anticipated to have strong effects on transition frequency. In any event the  $L \rightarrow M$  and  $M \rightarrow L$  charge transfer transition frequencies are expected to have greater solvent dependency than the d-d transition frequencies (i.e. radial electronic redistribution vs angular electronic redistribution). In the case of  $\text{PtCl}_4^{2-}$ , changing the solvent from  $\text{D}_2\text{O}$  to  $\text{CH}_3\text{CN}$  causes a red frequency shift of  $1000 \text{ cm}^{-1}$  in the ligand field transition  $b_{2g}^* \rightarrow b_{1g}^*$  which is increased to  $1710 \text{ cm}^{-1}$  for the  $e_u(\sigma^b) \rightarrow b_{1g}^*$  charge transfer transition. Presumably CTTS transitions would display the greatest solvent effects. Comparison of the blue frequency shifts in the bands of  $\text{PtCl}_4^{2-}$  and  $\text{Cl}^-$  on changing from  $\text{H}_2\text{O}$  to  $\text{D}_2\text{O}$  serves as an example. The  $b_{2u}(\pi^n) \rightarrow b_{1g}^*$ ,  $e_u(\pi^n) \rightarrow b_{1g}^*$ ,  $e_u(\sigma^b) \rightarrow b_{1g}^*$ , and  $e_g^* \rightarrow a_{2u}^*$  transitions are displaced 120, 180, 340, and  $590 \text{ cm}^{-1}$  respectively. It is only the tentatively assigned charge transfer from chloride ligand to solvent which experiences the same shift as that observed in the CTTS transition of uncomplexed chloride ion ( $\Delta\nu \approx 800 \text{ cm}^{-1}$ ).

An attempt has been made to define the envelope in which the study has been carried out by assigning both the highest and lowest frequency bands and then interpreting the intermediate spectral portion in an internally consistent manner. However it is important to realize that there is no guarantee that any spectrum contains all of the possible transitions within the accessible region.

The ligand field parameters,  $\Delta_1$ ,  $\Delta_2$ , and  $\Delta_3$  (Table XI), were calculated from the d - d spectra of the complexes using the following equations:<sup>1</sup>

$$\begin{aligned}
 E('A_{2g}) - E('A_{1g}) &= \text{observed spectral frequency of first} \\
 &\quad \text{d-d band.} \\
 &= \Delta_1 - C \\
 E('E_g) - E('A_{1g}) &= \Delta_1 + \Delta_2 - 3B - C \\
 E('B_{1g}) - E('A_{1g}) &= \Delta_1 + \Delta_2 + \Delta_3 - 4B - C \\
 &\quad \text{where } B = 500 \text{ cm}^{-1} \\
 &\quad \quad C = 3500 \text{ cm}^{-1}
 \end{aligned}$$

The values of the Racah interelectronic repulsion parameters, B and C, were chosen so as to agree with those used in the most recent publications<sup>8,14</sup>.

The energy ordering of the metal d orbitals has been well established<sup>6,7,8,13</sup> as  $b_{1g}^* > b_{2g}^* > e_g^* > a_{1g}^*$ . In  $d^8$  systems the latter three are fully occupied and  $b_{1g}^*$  is empty. The value of  $\Delta_1$  is usually larger than  $\Delta_2$  and  $\Delta_3$ . For a particular metal the magnitude of  $\Delta_1$  depends on the ligand:  $\text{CN}^- > \text{NH}_3 > \text{Cl}^- > \text{Br}^-$ . This is consistent with the ligand ordering in the octahedral spectrochemical series. The size of  $\Delta_1$  depends on the relative energies of  $b_{1g}^* (dx^2-y^2)_\sigma^*$  and  $b_{2g}^* (dxy)_\pi^*$ ; thus both  $\sigma$  and  $\pi$  bonding are significant factors. For a given ligand,  $\Delta_1$  depends on the nature of the metal ion. Specifically the splitting of the d-MO levels decreases as the central metal increases in oxidation number. For the sake of discussion it is convenient to compare Pt(II) and Pd(II), congeners in the periodic table, and to compare Pt(II) with Au(III), adjacent members in the same transition series.

A population analysis<sup>19</sup> of the d-MO levels calculated on the basis of a semiempirical MO treatment<sup>8</sup> suggests that the empty  $b_{1g}^*$ , a  $\sigma$  type, increases strongly in metal character (65% for  $\text{PtCl}_4^{2-}$  to 90% for

TABLE XI

## Ligand Field Parameters for Square Planar Complexes

Complex	$\Delta_1(\text{cm}^{-1})$	$\Delta_2(\text{cm}^{-1})$	$\Delta_3(\text{cm}^{-1})$
$\text{PtCl}_4^{2-}$	28,250	6250	8500
$[\text{PdCl}_4]$ in $\text{Pd}_2\text{Cl}_6^{2-}$	25,700	4240	a
$\text{AuCl}_4^{1-}$	25,430	6090	a
$\text{PtBr}_4^{2-}$	26,650	5230	3720
$[\text{PdBr}_4]$ in $\text{Pd}_2\text{Br}_6^{2-}$	20,450	3970	a
$\text{AuBr}_4^{1-}$	22,000	4320	a
$\text{Pt}(\text{CN})_4^{2-}$	55,730	4250	2240
$\text{Pd}(\text{CN})_4^{2-}$	44,500	3840	2920
$\text{Au}(\text{CN})_4^{1-}$	48,000	2630	1870

a Insufficient data



$\text{AuCl}_4^{1-}$ ) on increasing the oxidation number. The  $b_{2g}^*$ , a  $\pi$  type, shows a small increase in ligand character (50 % for  $\text{PtCl}_4^{2-}$  to 58% for  $\text{AuCl}_4^{1-}$ ). In other words, on going from Pt(II) to Au(III) the  $b_{1g}^*$  level experiences an energy decrease and the  $b_{2g}^*$  level a slight increase. Pd(II) shows the same general behaviour as Au(III) but on a reduced scale. The degree of ionic character of the three metals runs  $\text{Au(III)} \gg \text{Pd(II)} > \text{Pt(II)}$ . This order correlates nicely with the fact that both Au(III) and Pd(II) complexes undergo substitution reactions faster than Pt(II)<sup>28</sup>. The spectral results also agree nicely with this ordering:  $\Delta_1 [\text{Pt(II)}]$  is greater than both  $\Delta_1 [\text{Pd(II)}]$  and  $\Delta_1 [\text{Au(III)}]$ .

The replacement of chloride ligands by bromide ligands results in a weakening of both  $\sigma$  and  $\pi$  bonding. From the results of trans effect studies<sup>28</sup> bromide may be anticipated to have better  $\pi$  bonding, but the weakness of the  $\sigma$  bonding in bromide may be such that the  $\pi$  bonding is unable to take effect. In agreement with this, a red shift in  $\Delta_1$  (bromide) is observed for all of the complexes. In fact there is a general shrinkage of all three parameters  $\Delta_1$ ,  $\Delta_2$ , and  $\Delta_3$ , indicating an overall reduction of covalent bonding. This has been substantiated chemically by the observation that  $\text{PtBr}_4^{2-}$  does not have sufficient stability in water to yield a dependable electronic spectrum. On the other hand,  $\text{PtCl}_4^{2-}$  will give a reproducible spectrum over a short period of time. Again  $\Delta_1 [\text{Pt(II)}]$  is greater than either  $\Delta_1 [\text{Pd(II)}]$  or  $\Delta_1 [\text{Au(III)}]$ .

The cyanide ligand, not only a good  $\sigma$  and  $\pi$  bonder, but also a  $\pi$  acceptor, is able to raise the  $b_{1g}^*$  level through  $\sigma$  bonding and can also stabilize the  $b_{2g}^*$  level by  $d\pi \rightarrow \pi^* \text{CN}$  interaction. As a result, the magnitudes of  $\Delta_1 (\text{CN}^-)$  are greatly increased over those of  $\Delta_1 (\text{Cl}^-)$

and  $\Delta_1(\text{Br}^-)$ . Note again that the greater covalent character of Pt(II) places  $\Delta_1[\text{Pt(II)}]$  above  $\Delta_1[\text{Pd(II)}]$  and  $\Delta_1[\text{Au(III)}]$ .

The spectral frequencies of the various ligand to metal (L  $\rightarrow$  M) charge transfer transitions for a given ligand are a function of the relative energies of the  $b_{2u}(\pi^n)$ ,  $e_u(\pi^n)$ ,  $e_u(\sigma^b)$ , and  $b_{1g}^*(\sigma^*)$  levels. For a given metal the frequencies should relate to the relative electronegativities of the ligands.

A study of the chloride complexes of Pt(II) and Au(III) reveals that the L  $\rightarrow$  M charge transfer frequencies for Au(III) are lower than those for Pt(II). This correlates well with the increased oxidation number of Au(III). The bromide complexes of Pt(II) and Au(III) show the same spectral behaviour within the framework of an anticipated red shift. This can be attributed to the lower electronegativity of bromide and weaker  $\sigma$  bonding.

Before consideration of Pd(II) and Pt(II), attention should be drawn to the fact that the dimeric character of the Pd(II) chloride and bromide complexes splits the ligand levels into terminal and bridging sub-levels. The electron density from each bridging ligand is distributed over three centres whereas that of each terminal ligand is spread over two centres. Consequently the palladium-bridging ligand bonds would be anticipated to be weaker than the palladium-terminal ligand bonds. Thus the bridging ligand levels lie at relatively higher energies than the terminal ligand levels.

The previous analysis which attributed greater ionic character and weaker  $\sigma$  bonding to Pd(II) compared to Pt(II) applies once more in this case. The L  $\rightarrow$  M charge transfer frequencies of the Pd(II) chloride complex are lower than those of Pt(II). The bromide complexes of Pd(II)

and Pt(II) display identical behaviour but with an overall red shift expected on the basis of the chemical observation that bromide is more electropositive than chloride.

Ligand to metal (L → M) charge transfer transitions were not observed with the cyanide complexes. By any reasonable criteria they should occur at extremely high frequencies due to cyanide's high electronegativity, stronger  $\sigma$  bonding, anticipated stronger  $\pi$  bonding, and a lack of non-bonding electrons which are present in the halide complexes.

The spectral frequencies of the various metal to ligand (M → L) charge transfer transitions for a given ligand are a function of the relative energies of the  $b_{2g}^*$ ,  $e_g^*$ ,  $a_{1g}^*$ ,  $a_{2u}^*$ , and  $e_u^*$  levels. A population analysis<sup>8</sup> would suggest that the acceptor levels,  $a_{2u}^*$  and  $e_u^*$ , correlate mainly with the metal p orbital. Thus for a particular metal the frequencies may not be a strong function of the ligand electronegativity; the ligand  $\pi$  bonding may be of greater importance. On the other hand,  $\pi$  acceptor ligands such as cyanide have a strong influence on the transition frequencies because the  $d\pi \rightarrow \pi^*(CN)$  interaction can lower the  $b_{2g}^*(\pi^*)$  and  $e_g^*(\pi^*)$  levels.

The objection may be posed that from a chemical point of view the result of a M → L transition in a halide complex would have the following appearance:  $Pt^{+3} X^{-2}$ , a species of excessively high energy. On the other hand such a transition is commonly accepted for cyanide complexes,  $M(CN)_4^{n-}$ , due to the availability of  $\pi^*$  orbitals of relatively low energy. It is much easier to bear the thought of a M → L transition in a halide complex when recognition is made of the fact that the  $\pi^*$  of cyanide correlates with the nd promotion orbital in the simple halide ( $Cl^- 3d$ ,  $Br^- 4d$ ) via the united atom-separated atom approximation<sup>29</sup>.

Consideration of the chloride complexes of Pt(II) and Au(III) reveals that the  $M \rightarrow L$  charge transfer band of Au(III) occurs at higher frequency than that of Pt(II). This is to be expected on the basis of gold (III)'s larger oxidation number. Likewise the  $M \rightarrow L$  charge transfer transitions in the Au(III) bromide complex are shifted to the blue relative to the corresponding Pt(II) complex. The fact that the transitions in the bromide complexes occur at lower energy than those in the chloride complexes can be correlated with the shrinkage of energy level spacings at increasing nuclear distances. In other words, the 4d level of bromide is closer to the 4p level than the 3d level of chloride to its 3p level.

Comparison of the  $e_g^*$ ,  $a_{1g}^* \rightarrow a_{2u}^*$  and  $b_{2g}^*$ ,  $e_g^* \rightarrow e_u^*$  transition frequencies for the Pt(II) and Pd(II) complexes reveals that the transitions for Pt(II) occur at slightly higher frequencies than those for Pd(II). We observe this both in the case of the chloride ligands and to a lesser extent in the bromide ligands also. This can be interpreted as increased participation in bonding of the Pt 6p orbital over the Pd 5p orbital. Greater Pt 6p bonding compared to Pd 5p bonding would cause a proportionately larger increase in the energy of the  $a_{2u}^*$  and  $e_u^*$  levels. This correlates well with the observed split in energy of the  $\pi^n$  levels,  $b_{2u}$  and  $e_u$ , for the Pt(II) halides. It is also seen that the transitions in the bromide complexes of Pt(II) and Pd(II) are at lower energies than the corresponding ones in the chloride complexes. This is analogous to the Pt(II) - Au(III) comparison.

As stated before, the presence of the cyanide ligand can lower the  $b_{2g}^*(\pi^*)$  and  $e_g^*(\pi^*)$  levels by means of the  $d\pi \rightarrow \pi^*(CN)$  interaction.

It should be borne in mind that any observable result is a consequence of many factors, some of course of greater magnitude than others. In the cyanide complexes the final energies of the  $b_{2g}^*$  and  $e_g^*$  levels are the result of combining the  $d\pi \rightarrow \pi^*(CN)$  back-bonding interaction which lowers the levels and the cyanide  $\pi$  bonding which raises the levels. In comparing the  $M \rightarrow L$  charge transfer frequencies for the cyanide complexes of Pd(II) and Pt(II) it is noted that the transitions for Pt(II) occur at lower energy. It is convenient to interpret this in line with previously-made statements to the effect that Pt(II) complexes are generally more covalent than those of Pd(II). Not only does this greater covalent character raise the Pt  $b_{1g}^*(\sigma^*)$  level proportionately more than the Pd  $b_{1g}^*(\sigma^*)$  level  $\{\Delta_1[\text{Pt(II)}] > [\text{Pd(II)}]\}$ , but evidently it also raises Pt  $b_{2g}^*(\pi^*)$  and Pt  $e_g^*(\pi^*)$  by relatively greater amounts than Pd  $b_{2g}^*(\pi^*)$  and Pd  $e_g^*(\pi^*)$ . As a result the  $b_{2g}^*, e_g^*, a_{1g}^* \rightarrow a_{2u}^*, e_u^*$  transitions in Pt(II) occur at lower frequencies than the corresponding ones in Pd(II). It would appear that this is a case where cyanide  $\pi$  bonding predominates over the  $d\pi \rightarrow \pi^*(CN)$  interaction. This supports Mason and Gray's decision<sup>14</sup> to neglect the possibility of any strong  $d\pi \rightarrow \pi^*(CN)$  interaction. Their conclusion was based on infrared  $C \equiv N$  stretching frequencies for the complexes.

The  $M \rightarrow L$  charge transfer frequencies for  $\text{Au}(\text{CN})_4^{1-}$  are higher than those for  $\text{Pt}(\text{CN})_4^{2-}$ . This observation is consistent with gold (III)'s larger oxidation number.

As a crude approximation, the spectral properties of  $\text{Pt}(\text{en})\text{Cl}_2$  would be anticipated to lie somewhere between the limits set by  $\text{PtCl}_4^{2-}$  and  $\text{Pt}(\text{NH}_3)_4^{2+}$ . Table XII summarizes the published spectral frequencies and

TABLE XIIElectronic Spectrum<sup>14</sup> of Pt (NH<sub>3</sub>)<sub>4</sub><sup>2+</sup>

Frequency, cm <sup>-1</sup> X 10 <sup>-3</sup> (Extinction coefficient, M <sup>-1</sup> cm <sup>-1</sup> )		
H <sub>2</sub> O	CH <sub>3</sub> CN	<sup>1</sup> A <sub>1g</sub> →
34.97 (42.5)	34.60 (54)	<sup>3</sup> E <sub>g</sub> , <sup>3</sup> A <sub>2g</sub>
41.66 (143)	43.10 (191)	<sup>1</sup> A <sub>2g</sub> , <sup>1</sup> E <sub>g</sub>
45.25 (443)	46.08 (560)	<sup>1</sup> B <sub>1g</sub>
50.76 (11,070)	50.50 (12,300)	<sup>1</sup> E <sub>u</sub> (3)

assignments for  $\text{Pt}(\text{NH}_3)_4^{2+}$ . Ethylenediamine lies close to ammonia but just above it in the octahedral spectrochemical series. Thus they would be expected to be similar in behaviour. Generally the  $\sigma$  bonding in  $\text{Pt}(\text{en})\text{Cl}_2$  would be expected to be weaker than that in  $\text{Pt}(\text{NH}_3)_4^{2+}$  but stronger than that in  $\text{PtCl}_4^{2-}$ .

The frequencies for the ligand field transitions of  $\text{Pt}(\text{en})\text{Cl}_2$  in water ( $32,920 \text{ cm}^{-1}$ ,  $37,260 \text{ cm}^{-1}$ ) fit nicely above those of  $\text{PtCl}_4^{2-}$  ( $25,740 \text{ cm}^{-1}$ ,  $30,650 \text{ cm}^{-1}$ ,  $38,000 \text{ cm}^{-1}$ ) and below those of  $\text{Pt}(\text{NH}_3)_4^{2+}$  ( $41,660 \text{ cm}^{-1}$ ,  $45,250 \text{ cm}^{-1}$ ).

The net stronger  $\sigma$  bonding in  $\text{Pt}(\text{en})\text{Cl}_2$  should place the first  $L \rightarrow M$  charge transfer band ( $48,390 \text{ cm}^{-1}$ ) at higher frequency than the corresponding transition in  $\text{PtCl}_4^{2-}$  ( $43,200 \text{ cm}^{-1}$ ).

Note the frequency trend for the first  $d^* \rightarrow p^*$  type transition:  $\text{Pt}(\text{NH}_3)_4^{2+}$  ( $50,760 \text{ cm}^{-1}$ ),  $\text{Pt}(\text{en})\text{Cl}_2$  ( $53,030 \text{ cm}^{-1}$ ), and  $\text{PtCl}_4^{2-}$  ( $54,520 \text{ cm}^{-1}$ ). This can be correlated with increased participation of the 6 p orbital in bonding as the ligand is changed from  $\text{NH}_3$  to  $\text{Cl}^-$  and thus increased energy difference between metal  $d^*$  and metal  $p^*$  levels. This trend can be fitted neatly into a familiar qualitative scheme where  $\text{M}(\text{NH}_3)_4^{n+}$  with no  $\pi$  bonding is at one extreme and  $\text{MCl}_4^{m-}$  with its possibility of  $\pi$  bonding is at some intermediate point.

This research program was initiated to investigate the band structure in the  $1849 \text{ \AA}$  region of the electronic spectrum of aqueous  $\text{PtCl}_4^{2-}$ . The interpretation advanced here assigns the  $54,520 \text{ cm}^{-1}$  absorption to the  $M \rightarrow L e_g^* \rightarrow a_{2u}^*$  transition. The  $55,400 \text{ cm}^{-1}$  absorption remains an anomaly. At the outset of the investigation it was suspected to be a type of CTTS band, a charge transfer from a non-bonding ligand

orbital to the solvent. It is still tentatively assigned as such--tentative because the forever present problem of stray light introduces some uncertainty and also because of the lack of detailed photochemical data. However it is quite clear that solvated electrons are produced in the 1849 Å photolysis of aqueous  $\text{PtCl}_4^{2-}$ . The problem is how they are formed. A CTTS transition is a possible explanation. On the other hand the  $e_g^* \rightarrow a_{2u}^*$  transition can also be responsible: excitation of an electron to an orbital subjected to reduced effective nuclear charge followed by competition of the platinum complex and solvent for the electron. The outcome would depend on the relative electron affinities of the solvent and the complex in its excited state.

Unfortunately the correct assignment of the very interesting 55,400  $\text{cm}^{-1}$  band will likely remain a problem until the photochemistry has been studied in much deeper detail.



APPENDIX **I**

TABLE X111

<sup>8</sup>Electronic Spectra of PtCl<sub>4</sub><sup>2-</sup> and PdCl<sub>4</sub><sup>2-</sup>

Transition	Frequency, cm <sup>-1</sup> x 10 <sup>-3</sup> (extinction coefficient, M <sup>-1</sup> cm <sup>-1</sup> )	
	PtCl <sub>4</sub> <sup>2-a</sup>	PdCl <sub>4</sub> <sup>2-e</sup>
<sup>1</sup> A <sub>1g</sub> → <sup>3</sup> E <sub>g</sub>	17.0 (<1)z, 18.0(2)xy, 19.0(<1)z	d
→ <sup>3</sup> A <sub>2g</sub>	20.9(9)xy, 20.6(10)z	d
→ <sup>3</sup> B <sub>1g</sub>	24.0(7)xy, 24.1(3)z	18.0(19)xy, 17.0(7)z
→ <sup>1</sup> A <sub>2g</sub>	26.3(28)xy	20.0(67)xy
→ <sup>1</sup> E <sub>g</sub>	29.2(37)xy, 29.8(55)z	22.6(128)xy, 23.0(80)z
→ <sup>1</sup> B <sub>1g</sub>	36.5 <sup>b</sup>	29.5(67)xy
→ <sup>1</sup> A <sub>2u</sub> , <sup>1</sup> E <sub>u</sub> (1)	46.0(9580) <sup>c</sup>	36.0(12,000) <sup>f</sup>
→ <sup>1</sup> E <sub>u</sub> (2)	d	44.9(30,000) <sup>f</sup>

a Single-crystal absorption spectrum, K<sub>2</sub>PtCl<sub>4</sub>, 15°K

b Reflectance spectrum of K<sub>2</sub>PtCl<sub>4</sub>

c Aqueous solution spectrum of K<sub>2</sub>PtCl<sub>4</sub>

d Not reported

e Single-crystal absorption spectrum, K<sub>2</sub>PdCl<sub>4</sub>

f Aqueous solution spectrum of K<sub>2</sub>PdCl<sub>4</sub> with excess KCl

TABLE XIV

Electronic Spectra of Square Planar Halide Complexes<sup>14,19</sup>

Assignment	Frequency, $\text{cm}^{-1} \times 10^{-3}$ (extinction coefficient, $\text{M}^{-1} \text{cm}^{-1}$ ) <sup>a</sup>
$[(n\text{-C}_4\text{H}_9)_4\text{N}]_2 [\text{PtCl}_4]$	
${}^3\text{E}_g$	17.50 (6.5)
${}^3\text{A}_{2g}$	20.24 (16.6)
${}^1\text{A}_{2g}$	24.75 (59.6)
${}^1\text{E}_g$	29.50 (66.4)
${}^1\text{B}_{1g}$	37.03 (404)
${}^1\text{A}_{2u}, {}^1\text{E}_u(1)$	44.05 (26,900)
$[(n\text{-C}_4\text{H}_9)_4\text{N}]_2 [\text{Pt Br}_4]$	
${}^3\text{E}_g$	16.00 (9.3)
${}^3\text{A}_{2g}$	18.59 (25.0)
${}^1\text{A}_{2g}$	23.15 (126)
${}^1\text{E}_g$	26.88 (187)
${}^1\text{B}_{1g}$	30.03 (598)

TABLE XIV (contd.)

Electronic Spectra of Square Planar Halide Complexes<sup>14,19</sup>Assignment      Frequency,  $\text{cm}^{-1} \times 10^{-3}$  (extinction coefficient,  $\text{M}^{-1} \text{cm}^{-1}$ )<sup>a</sup>[(n-C<sub>4</sub>H<sub>9</sub>)<sub>4</sub>N]<sub>2</sub> [PtBr<sub>4</sub>] (contd.)

<sup>1</sup> A <sub>2u</sub>	33.33 (3860)
<sup>1</sup> E <sub>u(1)</sub>	36.04 (8400)
<sup>1</sup> E <sub>u(2)</sub>	47.38 (55,400)

[(n-C<sub>4</sub>H<sub>9</sub>)<sub>4</sub>N] [AuCl<sub>4</sub>]

<sup>1</sup> A <sub>2g</sub>	21.93 (17.3) <sup>b</sup>
<sup>1</sup> E <sub>g</sub>	25.00 (304)
<sup>1</sup> A <sub>2u</sub> , <sup>1</sup> E <sub>u(1)</sub>	31.05 (5020)
<sup>1</sup> E <sub>u(2)</sub>	44.25 (42,500)

[(n-C<sub>4</sub>H<sub>9</sub>)<sub>4</sub>N] [AuBr<sub>4</sub>]

<sup>1</sup> A <sub>2g</sub>	18.50 (119) <sup>b</sup>
<sup>1</sup> E <sub>g</sub>	21.74 (1560)
<sup>1</sup> A <sub>2u</sub> , <sup>1</sup> E <sub>u(1)</sub>	25.25 (4620.)
<sup>1</sup> E <sub>u(2)</sub>	39.06 (33,200)

TABLE XIV (contd.)

$[(n-C_4H_9)_4N]_2 [Pd_2Cl_6]$	
$^3A_{2g}$	16.29 (11.9) <sup>b</sup>
$^1A_{2g}$	22.20 (350)
$^1E_g$	24.94 (490)
$L_{\pi B} \rightarrow d\sigma^*$	30.00 (2100.)
$L_{\pi T} \rightarrow d\sigma^*$	34.70 (2260)
$L_{\sigma B} \rightarrow d\sigma^*$	40.98 (31,200)
$L_{\sigma T} \rightarrow d\sigma^*$	~ 50 (~70,000)
$[(n-C_4H_9)_4N]_2 [Pd_2Br_6]$	
$^3A_{2g}$	14.60 (15.1) <sup>b</sup>
$^1A_{2g}$	16.95 (74.8) <sup>b</sup>
$^1E_g$	20.60 (848)
$L_{\pi B} \rightarrow d\sigma^*$	24.27 (3470)
$L_{\pi T} \rightarrow d\sigma^*$	30.72 (4470)
$L_{\sigma B} \rightarrow d\sigma^*$	36.76 (36,000)
$L_{\sigma T} \rightarrow d\sigma^*$	46.30 (44,700)

a- Solvent  $CH_3CN$   
unless otherwise  
noted.

b- 2-Methyltetra-  
hydrofuran -  
propionitrile at  
77°K.

TABLE XV

Electronic Spectra of Square Planar Cyanide Complexes<sup>19,14</sup>

Assignment	Frequency, $\text{cm}^{-1} \times 10^{-3}$ (extinction coefficient, $\text{M}^{-1} \text{cm}^{-1}$ )		
	$\text{H}_2\text{O}^{\text{a}}$	$\text{CH}_3\text{CN}$	EPA <sup>b</sup> (77°K)
		$[(n\text{-C}_4\text{H}_9)_4\text{N}]_2 [\text{Pd}(\text{CN})_4]$	
${}^1\text{A}_{2g}$	41.66 (1100)	41.10 (1100)	41.41 (1260)
${}^1\text{B}_{1u}$			42.92 (1200)
${}^1\text{E}_u(3)$	45.45 (6800)	44.64 (6570)	44.31 (5700)
			45.09 (9800)
${}^1\text{A}_{2u}$	47.17 (8400)	46.73 (11,800)	46.19 (9200)
${}^1\text{E}_u(4)$	49.00 (10,400)	47.60 (10,700)	
		$[(n\text{-C}_4\text{H}_9)_4\text{N}]_2 [\text{Pt}(\text{CN})_4]$	
${}^1\text{B}_{1u}$	35.70 (1270)	35.34 (1270)	35.60 (2430)
${}^1\text{E}_u(3)$	39.00 (9000)	38.31 (13,200)	38.39 (11,950)
			39.25 (15,460)
${}^1\text{A}_{2u}$	41.30 (1300)	40.50 (1820)	41.41 (2740)
${}^1\text{E}_u(4)$	46.19 (18,700)	45.45 (29,400)	46.19 (32,200)
		$[(n\text{-C}_4\text{H}_9)_4\text{N}] [\text{Au}(\text{CN})_4]$	
	> 54.00	> 54.00	

a for  $\text{K}_2\text{M}(\text{CN})_4$

b Ether--isopentane--ethanol

TABLE XVI

Comparison of Computed and Observed Spectral Band Frequencies<sup>a,10</sup>

Transition	PtCl <sub>4</sub> <sup>2-</sup>		PtBr <sub>4</sub> <sup>2-</sup>		PDCl <sub>4</sub> <sup>2-</sup>		PDBr <sub>4</sub> <sup>2-</sup>		AuCl <sub>4</sub> <sup>1-</sup>		AuBr <sub>4</sub> <sup>1-</sup>	
	obs.	calc.	obs.	calc.	obs.	calc.	obs.	calc.	obs.	calc.	obs.	calc.
<sup>1</sup> A <sub>1g</sub> → <sup>3</sup> A <sub>2g</sub>	20.3	19.4		16.9		12.8		11.6				
→ <sup>3</sup> E <sub>g</sub>	18.0	17.8	16.7	16.5		11.7		9.6				
→ <sup>3</sup> B <sub>1g</sub>	23.6	25.7	19.7	20.9		17.5		11.9				
→ <sup>1</sup> A <sub>2g</sub>	26.7	25.2	24.3	23.3	20.0	20.0	16.0	18.2				
→ <sup>1</sup> E <sub>g</sub>	29.0	29.4		25.7	22.8	22.3	20.0	19.3				
→ <sup>1</sup> B <sub>1g</sub>	36.5	36.7	28.2	31.0	29.5	26.6	21.7	22.6				
→ <sup>1</sup> A <sub>2g</sub> (1)	46.0	b	37.3	b	36.0	b	30.1	b	32.1	b	26.4	b
→ <sup>1</sup> E <sub>u</sub> (2)	c	58.0	c	50.7	44.9	48.9	40.5	44.0	44.2	43.9	39.4	38.9

a energies in 1000 cm<sup>-1</sup>

b fitted

c not reported

## APPENDIX II

MCD has been demonstrated<sup>17</sup> to be a powerful tool in analyzing electronic absorption spectra. By evaluating the Faraday parameters A, B, and C (see references 32 and 33 for detailed descriptions of these parameters) considerable insight can be gained in elucidating the orbital degeneracies of the ground state and excited states. Since  $C = 0$  for a non-degenerate ground state, then only A terms (non-zero when either the ground state or excited states are orbitally degenerate) and B terms (which occur for all states regardless of degeneracy) are possible for diamagnetic  $d^8$  complexes.

The presence of an A term and hence an  $E_u$  excited state ( $E_u$  is the only parity allowed orbitally degenerate state possible in  $D_{4h}$  symmetry) is manifested by a change in the sign of  $(\theta)_M$  corresponding to an absorption maximum in the absorption spectrum. While Piepho, Schatz, and McCaffery<sup>30</sup> (PSM) have observed three apparent A terms at 35,800, 39,200 and 46,100  $\text{cm}^{-1}$ , they could not associate these with pure  $E_u$  excited states and were thus prompted to explain their results by invoking pseudo-A terms formed via spin-orbit coupling. The bands at 46,100  $\text{cm}^{-1}$  and 39,200  $\text{cm}^{-1}$  were assigned to composite  $A_{1g} \rightarrow (A'_{2u} + E'_u)$  transitions and that at 35,800  $\text{cm}^{-1}$  to  $A_{1g} \rightarrow E'_u$  where the prime (') refers to double group states derived from the spin-forbidden triplet states  ${}^3A_{2u} (a_{1g}^* \rightarrow a_{2u}^*)$ ,  ${}^3E_u (e_g^* \rightarrow a_{2u}^*)$ , and  ${}^3B_{1u} (b_{2g}^* \rightarrow a_{2u}^*)$ .

Although this interpretation of the ultraviolet spectrum of  $\text{Pt}(\text{CN})_4^{2-}$  rationalizes the MCD data, it would seem premature to abandon the alternate assignment proposed here or by Mason and Gray<sup>14</sup> for the following reasons:



(a) the MCD data is by no means unambiguous since the A terms used by PSM were derived only by extensive calculations involving numerous approximations including the use of pure d-orbital wave functions and strong Pt spin-orbit coupling in a molecule of unquestionably strong covalent character.

(b) the resultant ordering of the d-orbitals as  $dx^2 - y^2 > dz^2 > dxz, dyz > dxy$  completely contradicts any order yet established for a  $d^8$  metal in  $D_{4h}$  symmetry. 6, 7, 8, 10, 13, 14, 15, 16, 20, 21, 27

(c) of the six transitions clearly observed in this region only four are accounted for by PSM. Using similar arguments based on spin-orbit coupling or distortions to Td symmetry in the excited state,<sup>14</sup> it would appear possible to account for the MCD data using the assignments presented here. However in the absence of the contingent detailed calculations this assertion must remain speculative.

## BIBLIOGRAPHY

1. Lever, A.B.P. Inorganic Electronic Spectroscopy. Monograph 1 of Physical Inorganic Chemistry, ed. M.F. Lappert. New York: Elsevier, 1968.
2. Smith, M., and M.C.R. Symons. Trans. Far. Soc. 54, 338 (1958) and subsequent papers.
3. Airey, D.L., and F.S. Dainton. Proc. Roy. Soc. A291, 340 (1966).
4. Balzani, V., L. Moggi, and V. Carassiti. Deutsche Bunsengesellschaft Für Physikalische Chemie Berichte 72 (2), 288 (1968).
5. Balzani, V., and V. Carassiti. J. Phys. Chem. 72, 383 (1968).
6. Martin, D.S., Jr., M.A. Tucker, and A.J. Kassman. Inorg. Chem. 4, 1682 (1965).
7. Martin, D.S., Jr., M.A. Tucker, and A.J. Kassman. Inorg. Chem. 5, 1298 (1966).
8. Basch, H., and H.B. Gray. Inorg. Chem. 6, 365 (1967).
9. Adamson, A.W., et al. Chemical Reviews 68, 541 (1968).
10. Basch, H. Ph.D. Thesis. Columbia University. 1967.
11. Figgis, B.N. Introduction to Ligand Fields. New York: Interscience, 1966.
12. Kauzmann, W. Quantum Chemistry. New York: Academic Press, 1964.
13. Cotton, F.A., and C.B. Harris. Inorg. Chem. 6, 369 (1967).
14. Mason, W.R., and H.B. Gray. J. Am. Chem. Soc. 90, 5721 (1968).
15. Martin, D.S., Jr., and C.A. Lenhardt. Inorg. Chem. 3, 1368 (1964).
16. Martin, D.S., Jr., et al. Inorg. Chem. 5, 491 (1966).
17. McCaffery, A.J., P.N. Schatz, and P.J. Stephens. J. Am. Chem. Soc. 90, 5730 (1968).
18. Day, P., et al. J. Chem. Phys. 42, 1973 (1965).
19. Mason, W.R., and H.B. Gray. Inorg. Chem. 7, 55 (1968).

20. Fenske, R.F., D.S. Martin, Jr., and K. Ruedenberg. Inorg. Chem. 1, 441 (1962).
21. Gray, H.B., and C.J. Ballhausen. J. Am. Chem. Soc. 85, 260 (1963).
22. Smith, J.M., et al. Inorg. Chem. 4, 369 (1965).
23. Jorgensen, C.K. Acta. Chem. Scand. 10, 518 (1956).
24. Blandamer, M.J., et al. Trans. Far. Soc. 60, 1524 (1964).
25. Berry, R.S., C.W. Reiman, and G.N. Spokes. J. Chem. Phys. 37, 2278 (1962).
26. Cotton, F.A. Chemical Applications of Group Theory. New York: Interscience, 1964.
27. Chatt, J., G.A. Gamlen, and L.E. Orgel. J. Chem. Soc. 486 (1958).
28. Basolo, F., and R.G. Pearson. Mechanisms of Inorganic Reactions, 2nd ed. New York: John Wiley and Sons, 1967.
29. King, G.W. Spectroscopy and Molecular Structure. Toronto: Holt, Rinehart and Winston, 1964.
30. Piepho, S.B., P.N. Schatz, and A.J. McCaffery. J. Am. Chem. Soc. 91, 5994 (1969).
31. Professor D.S. Martin, Jr. Personal Communication.
32. Schatz, P.N., et al. J. Chem. Phys. 45, 722 (1966).
33. Buckingham, A.D., and P.J. Stephens. Ann. Rev. Phys. Chem. 17, 399 (1966).

VITA AUCTORIS

Born:

April 4, 1943; Windsor, Ontario, Canada. Son of Mr. Frederick and Mrs. Gracia Batiste.

Primary School:

J. E. Benson, Windsor, Ontario, Canada,

Secondary School:

Assumption High School, Windsor, Ontario, Canada.  
Academic course: 1957 - 1962.

University:

University of Windsor, Windsor, Ontario, Canada.  
1962 - 1970. Degrees: B.Sc. Honours Chemistry - 1966.  
M.Sc. Chemistry - 1968.

Awards:

1962 - 63: Windsor and District Labour Council Bursary  
1963 - 66: University of Windsor In-Course Scholarships  
1965 - 66: Royal Canadian Institute Scholarship  
1964 - 65: Board of Governors Medal for III Year  
1965 - 66: Board of Governors Medal for Chemistry  
1966: Governor-General's Medal  
1966: Award of American Institute of Chemists  
1966: Hon. Mention - Woodrow Wilson Fellowship Competition  
1966 - 67: National Research Council of Canada Bursary  
1967 - 70: National Research Council of Canada Studentship.

Publication:

Can. J. Chem. 47, 4073 (1969): "New Approach to the Synthesis of Optically Active Trityl Systems".

Marital Status:

Married June 14, 1969 to Mary Margaret Shaw.